

## On the Gamma-limit of joint image segmentation and registration functionals based on phase fields

BENEDIKT WIRTH

*Institute for Computational and Applied Mathematics and  
Cells-in-Motion Cluster of Excellence (EXC 1003 – CiM),  
University of Münster, Einsteinstraße 62, 48149 Münster, Germany  
E-mail: benedikt.wirth@uni-muenster.de*

[Received 25 June 2015 and in revised form 28 May 2016]

A classical task in image processing is the following: Given two images, identify the structures inside (for instance detect all image edges or all homogeneous regions; this is called segmentation) and find a deformation which maps the structures in one image onto the corresponding ones in the other image (called registration). In medical imaging, for instance, one might segment the organs in two patient images and then identify corresponding organs in both images for automated comparison purposes. The image segmentation is classically performed variationally using the Mumford–Shah model, and the obtained structures are then mapped onto each other by minimizing a registration energy in which the deformation is regularized via elasticity. Experimentally it often seems more robust to perform segmentation and registration simultaneously so that both can benefit from each other. The question to be examined here is how phase field approximations of the Mumford–Shah model behave if used for the joint segmentation and registration problem. We mathematically analyze corresponding generic phase field models and reveal interesting phenomena that rule out some of the models. These phenomena are characteristic of coupling phase fields with deformations and thus are interesting in their own right. In essence, region-based segmentation and registration problems can well be approximated using phase fields, while edge-based approaches typically suffer from different types of vanishing or newly appearing edges. We conjecture how the introduction of a different scaling could remedy those shortcomings.

*2010 Mathematics Subject Classification:* Primary 49J45; Secondary 49N45.

*Keywords:* Image segmentation, image registration, phase fields, Mumford–Shah.

### 1. Introduction

In various applications (most prominently computational anatomy [6, 17]), two given images  $\hat{y}_0, \hat{y}_1 : \Omega \rightarrow \mathbb{R}$ ,  $\Omega \subset \mathbb{R}^d$ , have to be registered, i.e. a deformation  $\phi : \Omega \rightarrow \mathbb{R}^d$  is sought such that the pullback  $\hat{y}_0 \circ \phi$  looks like  $\hat{y}_1$  or at least maps the structures visible in image  $\hat{y}_0$  onto the corresponding ones in image  $\hat{y}_1$  (Fig. 1, cf. also Figs. 2, 3). To reduce the influence of noise in the images and to facilitate the registration of the encoded structures, these structures (e.g. image edges or homogeneous regions) can be extracted first (so-called image segmentation) so that the registration deformation  $\phi$  only has to map the structures from one image onto the corresponding ones of the other.

The most widely used model for variational segmentation of an image into edges and piecewise smooth or constant regions dates back to the work of Mumford and Shah [30], and classical phase field and level set approximations include the approaches by Ambrosio and Tortorelli [2] and

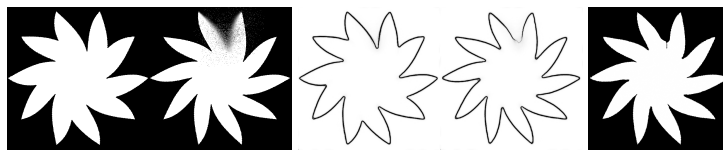


FIG. 1. Joint edge segmentation and registration of two input images from the MPEG7 shape database (left) leads to detected edge sets (middle) and a matching deformation (the rightmost image shows the registered image  $\hat{y}_0 \circ \phi$ ). Note that some weak edges in the second image have been restored based on the edge information from the first image. Results have actually been computed using an Ambrosio–Tortorelli phase field approximation.

by Chan and Vese [14]. Alternative variational approaches include active contour-type methods, e.g. [9], which seek a closed curve coinciding with image edges, and graph cut-based ideas, e.g. [41], in which the problem is typically reformulated as a segmentation of a discrete graph. More recently, convex approximations to the Mumford–Shah segmentation problem became popular [13, 29], where a solution to the original segmentation problem can be obtained from solving a convex problem in a higher-dimensional space.

Image registration has an equally long history. Already in the 90’s, matching deformations between images were sought by minimizing a data term and a regularizing deformation energy such as linearized elasticity [18, 24, 27] or viscous fluid regularization [10, 15–17, 26]. Regularization via optimal transport [37, 42] is also possible but much weaker, since it does not penalize higher order norms of the deformation. A hyperelastic regularization is particularly appropriate for large deformations [20, 21, 31, 34] and can also be used to encode additional nonlinear constraints such as mass preservation [12].

It has often been observed and exploited that segmentation and registration can benefit from each other if performed simultaneously [21, 23, 35, 36, 39, 40]: The registration becomes simpler if applied to cleanly segmented regions, and conversely the segmentation can use information from both images if they are already registered. Indeed, the latter is exploited in [25, 31, 32] to achieve a registration-based segmentation via the transfer of edges from a template to a reference image. Moreover, weak edges in one of the images can even be automatically restored based on a registration (Fig. 1). As for the positive effect of segmentation on registration, clearly outlined segmented structures can reliably drive the registration and thereby also provide good deformation estimates in between those structures, a property important for atlas-based medical image segmentation [4, 22]. To give an example from a slightly different context, a positive mutual influence is also observed in joint image reconstruction and motion estimation [7]. Yet a different approach, with a flavor similar to the models we shall consider, consists in a joint optical flow estimation with phase field segmentation of the flow field [11].

This work is concerned with the class of methods from the previous paragraph, that aim at a simultaneous image segmentation and registration. In particular, we will examine how phase field approximations to the Mumford–Shah segmentation model behave in this context, where for the registration part we use the strongest of the above-mentioned regularizations, a hyperelastic energy. Our analysis for instance also covers the joint phase field segmentation and registration models from [21, 23].

In detail, there are essentially two phase field approximations for the Mumford–Shah model: The Modica–Mortola approximation [28], in which the phase field encodes the homogeneous image regions, and the Ambrosio–Tortorelli approximation [2], in which the phase field encodes the image

edges. If one combines the phase field segmentation functionals with an image registration term, in which the matching deformation is regularized via a hyperelastic energy, then the following can be observed: As the phase field parameter  $\varepsilon$  tends to zero, the joint segmentation and registration functional based on Modica–Mortola phase fields  $\Gamma$ -converges exactly against the expected sharp interface limit and thus represents a feasible model (cf. Thm. 4.1). Using Ambrosio–Tortorelli phase fields, however, we see three distinct effects, the first two already in 1D:

1. The phase field profile is squeezed by the matching deformation so that part of the phase field will be ignored (cf. Thms. 4.3, 4.5, and 4.7).
2. Spurious ghost phase fields occur which in the  $\Gamma$ -limit change the originally intended weights in the energy (cf. Thms. 4.5, 4.6, and 4.7).
3. In 2D, a string of phase field dots can be dilated tangentially to the phase field representation of an edge, ultimately resulting in the lack of any registration in the  $\Gamma$ -limit (cf. Ex. 4.8).

As for the second item above we will argue that, though perhaps unexpected at first glance, this behavior is desirable and in fact is a manifestation of the edge restoration property that joint segmentation and registration methods possess (cf. Fig. 1). We will also put forward suggestions how the first and last item can be remedied by slight modifications of the joint segmentation and registration functionals; the detailed analysis of these modifications will be reserved for future work.

Note that even though our presentation restricts to an image processing application, the described phenomena are not limited to that application and are to be expected whenever phase fields are composed with deformations.

The article is organized as follows. After some notations in Sec. 2, Sec. 3 briefly introduces Mumford–Shah-type segmentation functionals and associated joint segmentation and registration models. The corresponding phase field approximations are given in Sec. 4. This section also states our main results, the  $\Gamma$ -limits of the respective energies for  $\varepsilon \rightarrow 0$ , which formalize the above-described phenomena. Furthermore, a discussion of improvements to the functionals is provided in that section. The proofs of the limits are collected in Sec. 5.

## 2. Notations and assumptions

In the following,  $\Omega \subset \mathbb{R}^d$  ( $d = 1, 2, 3$ ) denotes a bounded, connected, (strongly) Lipschitz domain. We denote the Lebesgue space on  $\Omega$  with exponent  $p$  by  $L^p(\Omega)$  and the Sobolev space of functions in  $L^p(\Omega)$  with weak derivatives in  $L^p(\Omega)$  by  $W^{1,p}(\Omega)$ . The prefix  $w$ - as in  $w$ - $W^{1,p}(\Omega)$  stands for a Lebesgue or Sobolev space equipped with the weak topology, and  $\text{pw-}W^{1,2}(\Omega)$  for  $\Omega \subset \mathbb{R}^1$  shall be the space of functions on  $\Omega$  which are piecewise  $W^{1,2}$ . Also, we define  $W_{\text{id}}^{1,p}(\Omega) = \{\phi \in (W^{1,p}(\Omega))^d : \phi|_{\partial\Omega} = \text{id}\}$ , where  $\phi|_{\partial\Omega}$  is the trace of  $\phi$  on  $\partial\Omega$  and  $\text{id}$  is the identity function. For a piecewise continuous image  $y : \Omega \rightarrow \mathbb{R}$ , we denote by  $\mathcal{S}_y \subset \Omega$  its discontinuity set. Finally, for a matrix  $A \in \mathbb{R}^{d \times d}$ ,  $\|A\|_F = \sqrt{\text{tr}(A^T A)}$  shall be its Frobenius norm and  $\text{cof}A$  its cofactor matrix ( $\text{cof}A = \det AA^{-T}$  for invertible  $A$ ).

For simplicity we will assume  $\hat{y}_0, \hat{y}_1 \in L^\infty(\Omega)$  for the given images  $\hat{y}_0, \hat{y}_1$  to be matched. For the regularization of the matching deformation inside the joint segmentation and registration functionals we will consider the hyperelastic energy  $\mathcal{W}[\phi] = \int_\Omega W(\mathfrak{D}\phi) \, dx$ , where  $\mathfrak{D}\phi : \Omega \rightarrow \mathbb{R}^{d \times d}$  denotes the (weak) derivative of  $\phi$ . We will assume the following classical conditions to hold for its energy density  $W$  (cf. [33, Secs. 2.1 & 3.4]),

1. for all  $A \in \mathbb{R}^{d \times d}$  and  $U, O \in \text{SO}(d)$  we have  $W(UAO) = W(A)$ ,
2. the set of global minimizers of  $W$  is given by  $\text{SO}(d)$  with minimum value 0,

3.  $W(A) = \infty$  for  $\det(A) \leq 0$  and  $W(A) \rightarrow \infty$  as  $\det A \rightarrow 0$  or  $\det A \rightarrow \infty$ ,
4.  $W$  is polyconvex,
5. for all  $A \in \mathbb{R}^{d \times d}$  we have  $W(A) \geq C_1(\|A\|_F^p + \|\operatorname{cof} A\|_F^q + |\det A|^{-s}) - C_2$  for some  $C_1, C_2 > 0$ ,  $p, q > d$ , and  $s > \frac{(d-1)q}{q-d}$ , and
6. for some  $C_1, C_2, r > 0$ ,  $W(A) \leq C_1(\|A\|_F^r + |\det A|^r + |\det A|^{-r}) + C_2 \forall A \in \mathbb{R}^{d \times d}$ .

Condition 1 expresses the frame indifference or rigid body motion invariance of the deformation energy as well as the assumption of an isotropic underlying material. Condition 2 means that isometric deformations  $\phi$  cost no energy, and condition 3 implies infinite deformation energy for self-penetration of the deformed material. Finally, condition 4 in combination with condition 5 ensures the sequential weak lower semi-continuity of  $\mathcal{W}$  in  $W^{1,p}(\Omega)$  (smaller exponents in condition 5 would actually suffice [33, Thms. 3.5-3.6]), and condition 5 implies that deformations  $\phi \in W_{\text{id}}^{1,p}(\Omega)$  with a finite energy are Hölder continuous homeomorphisms with Hölder continuous inverse, as will briefly be derived below. Condition 6 just bounds the growth of the energy density and can easily be replaced by different growth conditions, leading to corresponding small changes of the results. Typical densities have the form  $W(A) = \alpha_1 \|A\|_F^p + \alpha_2 \|\operatorname{cof} A\|_F^q + \alpha_3 |\det A|^{-s} + \alpha_4$ .

Note that due to  $|\det A| \leq d! \|A\|_F^d$  condition 5 automatically implies  $W(A) \geq C_1 |\det A|^{p/d} - C_2$  so that a finite energy  $\mathcal{W}[\phi]$  also implies a Sobolev bound for the determinant  $\det \mathfrak{D}\phi$ . The fact that, under condition 5, deformations  $\phi \in W_{\text{id}}^{1,p}(\Omega)$  with finite energy are Hölder continuous and have a Hölder continuous inverse follows from the Sobolev embeddings  $W^{1,p}(\Omega) \subset C^{0,1-d/p}(\bar{\Omega})$ ,  $W^{1,\tilde{q}}(\Omega) \subset C^{0,1-d/\tilde{q}}(\bar{\Omega})$  and the following result by Ball, applied for  $\phi_0 = \text{id}$  and  $\tilde{q} = q \frac{1+s}{q}$ .

**Theorem 2.1** ([5, Thm. 2]) *Let  $\Omega \subset \mathbb{R}^d$  be a nonempty bounded connected strongly Lipschitz open set. Let  $\phi_0 : \bar{\Omega} \rightarrow \mathbb{R}^d$  be continuous in  $\bar{\Omega}$  and one-to-one in  $\Omega$  such that  $\phi_0(\Omega)$  satisfies the cone condition. Let  $p > d$  and let  $\phi \in W^{1,p}(\Omega)^d$  satisfy  $\phi|_{\partial\Omega} = \phi_0|_{\partial\Omega}$  and  $\det \mathfrak{D}\phi > 0$  almost everywhere. Suppose that for some  $\tilde{q} > d$ ,*

$$\int_{\Omega} \|\mathfrak{D}\phi(x)^{-1}\|_F^{\tilde{q}} \det \mathfrak{D}\phi(x) \, dx < \infty.$$

*Then  $\phi$  is a homeomorphism of  $\Omega$  onto  $\phi_0(\Omega)$ , and the inverse function  $x(\phi)$  belongs to  $W^{1,\tilde{q}}(\phi_0(\Omega))^d$ . The matrix of weak derivatives of  $x(\cdot)$  is given by  $\mathfrak{D}x(v) = \mathfrak{D}\phi(x(v))^{-1}$  for almost every  $v \in \phi_0(\Omega)$ . If, further,  $\phi_0(\Omega)$  is strongly Lipschitz, then  $\phi$  is a homeomorphism of  $\bar{\Omega}$  onto  $\phi_0(\bar{\Omega})$ .*

Note that, denoting by  $|\Omega|$  the Lebesgue volume of  $\Omega$ , the above integrability condition holds due to

$$\begin{aligned} \int_{\Omega} \|(\mathfrak{D}\phi)^{-1}\|_F^{\tilde{q}} \det \mathfrak{D}\phi \, dx &= \int_{\Omega} \|\operatorname{cof} \mathfrak{D}\phi\|_F^{\tilde{q}} (\det \mathfrak{D}\phi)^{1-\tilde{q}} \, dx \\ &\leq \left( \int_{\Omega} \|\operatorname{cof} \mathfrak{D}\phi\|_F^q \, dx \right)^{\frac{\tilde{q}}{q}} \left( \int_{\Omega} (\det \mathfrak{D}\phi)^{q \frac{1-\tilde{q}}{q}} \, dx \right)^{\frac{q-\tilde{q}}{q}} \\ &\leq \frac{1}{C_1} (\mathcal{W}[\phi] + C_2 |\Omega|)^{\frac{\tilde{q}}{q}} (\mathcal{W}[\phi] + C_2 |\Omega|)^{\frac{q-\tilde{q}}{q}} < \infty. \end{aligned}$$

### 3. Mumford–Shah-based image segmentation and registration

Here we introduce the binary as well as the original Mumford–Shah segmentation energy, together with the joint segmentation and registration framework.

#### 3.1 Region-based image segmentation and registration

Region-based image segmentation is classically performed by minimizing the binary Mumford–Shah functional [14]

$$\mathcal{E}_{\text{bMS}}^{\hat{y}}[(\underline{c}, \bar{c}), \mathcal{O}] = \alpha \int_{\mathcal{O}} |\underline{c} - \hat{y}|^2 dx + \alpha \int_{\Omega \setminus \mathcal{O}} |\bar{c} - \hat{y}|^2 dx + \nu \mathcal{H}^{d-1}(\partial^* \mathcal{O} \cap \Omega),$$

which segments a given image  $\hat{y}$  into two regions  $\mathcal{O}$  and  $\Omega \setminus \mathcal{O}$  with average gray values  $\underline{c}, \bar{c} \in \mathbb{R}$  ( $\alpha, \nu > 0$  are fixed weights,  $\partial^* \mathcal{O}$  denotes the essential boundary [1, Def. 3.62] and  $\mathcal{H}^{d-1}$  the  $(d-1)$ -dimensional Hausdorff measure). The registration of segmented regions  $\mathcal{O}_0, \mathcal{O}_1$  from two different images can now be obtained by minimizing  $a \mathcal{F}_{\text{vol}}[\mathcal{O}_0, \mathcal{O}_1, \phi] + \mathcal{W}[\phi]$  for the matching deformation  $\phi$ , where

$$\mathcal{F}_{\text{vol}}[\mathcal{O}_0, \mathcal{O}_1, \phi] = \text{vol}(\mathcal{O}_1 \Delta \phi^{-1}(\mathcal{O}_0)),$$

represents a mismatch penalty (with  $\Delta$  denoting the symmetric difference) which is weighted by  $a > 0$ , and the nonlinear hyperelastic energy

$$\mathcal{W}[\phi] = \int_{\Omega} W(\mathfrak{D}\phi) dx$$

serves as a regularization of the deformation (cf. [12, 20, 21, 34]). The elastic energy density  $W$  shall satisfy the conditions from the previous section. The joint region- or volume-based segmentation and registration functional for the two input images  $\hat{y}_0, \hat{y}_1$  thus reads

$$\begin{aligned} \mathcal{J}_{\text{vol}}[(\underline{c}_0, \bar{c}_0), (\underline{c}_1, \bar{c}_1), \mathcal{O}_0, \mathcal{O}_1, \phi] \\ = \mathcal{E}_{\text{bMS}}^{\hat{y}_0}[(\underline{c}_0, \bar{c}_0), \mathcal{O}_0] + \mathcal{E}_{\text{bMS}}^{\hat{y}_1}[(\underline{c}_1, \bar{c}_1), \mathcal{O}_1] + a \mathcal{F}_{\text{vol}}[\mathcal{O}_0, \mathcal{O}_1, \phi] + \mathcal{W}[\phi]. \end{aligned}$$

Fig. 2 shows an example of a region-based joint segmentation and registration. The result is well acceptable, even though the hyperelastic energy density employed in the numerical calculation,  $W(A) = \frac{1}{2} \|A\|_F^2 + \frac{1}{4} |\det A|^2 - \frac{3}{2} \log \det A - \frac{5}{4}$ , only satisfies weaker conditions than demanded in Sec. 2. The discretization of  $\phi$  is here based on bilinear finite elements. By choosing quadrature points at the mesh vertices,  $\det \mathfrak{D}\phi > 0$  is ensured everywhere, since a  $\phi$  with  $\det \mathfrak{D}\phi \leq 0$  within any element would yield infinite energy during the iterative optimization and is just discarded as an optimization step.

#### 3.2 Edge-based image segmentation and registration

As an alternative to using the homogeneous image regions one can identify and register all image edges. The classical corresponding segmentation functional is given by the Mumford–Shah energy [30]

$$\mathcal{E}_{\text{MS}}^{\hat{y}}[y, \mathcal{S}_y] = \int_{\Omega \setminus \mathcal{S}_y} |\nabla y|^2 + \alpha |y - \hat{y}|^2 dx + \nu \mathcal{H}^{d-1}(\mathcal{S}_y),$$

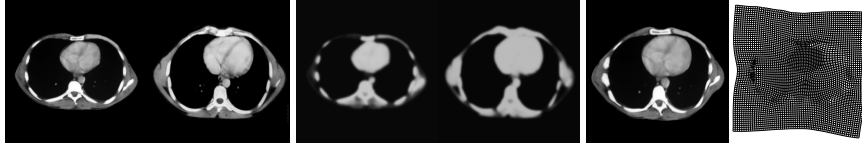


FIG. 2. Left: Two thorax CT-scans  $\hat{y}_0, \hat{y}_1$  to be registered. Middle: Binary segmentation results  $\mathcal{O}_0, \mathcal{O}_1$  for both CT-scans (colored with the gray values obtained during segmentation). Right: Pullback  $\hat{y}_0 \circ \phi$  as well as  $\phi$ , where the registration deformation  $\phi$  is computed based on matching the segmentation regions. Results are actually obtained via simultaneous variational segmentation and registration, using a Modica–Mortola phase field description of the regions  $\mathcal{O}_0, \mathcal{O}_1$ . These phase fields (both middle images) can be thought of as a smoothed version of the characteristic functions of  $\mathcal{O}_0, \mathcal{O}_1$  (which is the reason why they are not exactly binary).

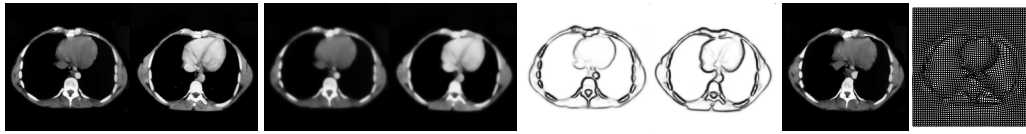


FIG. 3. Left: Two thorax CT-scans  $\hat{y}_0, \hat{y}_1$  to be registered. Middle: Mumford–Shah segmentation results (piecewise smooth approximations  $y_0, y_1$  and edge sets  $\mathcal{S}_{y_0}, \mathcal{S}_{y_1}$ ) for both CT-scans. Right: Pullback  $\hat{y}_0 \circ \phi$  as well as  $\phi$ , where the registration deformation  $\phi$  is computed based on matching the image edge sets. Results are actually obtained via simultaneous variational segmentation and registration, using an Ambrosio–Tortorelli phase field description of the edge sets  $\mathcal{S}_{y_0}, \mathcal{S}_{y_1}$  (which is the reason why both edge sets appear a little diffuse).

whose minimization yields a piecewise smooth approximation  $y$  to the given image  $\hat{y}$  as well as the corresponding edge set  $\mathcal{S}_y$ . Using a mismatch penalty

$$\mathcal{F}_{\text{edge}}[\mathcal{S}_{y_0}, \mathcal{S}_{y_1}, \phi] = \mathcal{H}^{d-1}(\mathcal{S}_{y_1} \Delta \phi^{-1}(\mathcal{S}_{y_0})),$$

a joint edge-based segmentation and registration functional is obtained by

$$\mathcal{J}_{\text{edge}}[y_0, y_1, \mathcal{S}_{y_0}, \mathcal{S}_{y_1}, \phi] = \mathcal{E}_{\text{MS}}^{\hat{y}_0}[y_0, \mathcal{S}_{y_0}] + \mathcal{E}_{\text{MS}}^{\hat{y}_1}[y_1, \mathcal{S}_{y_1}] + a\mathcal{F}_{\text{edge}}[\mathcal{S}_{y_0}, \mathcal{S}_{y_1}, \phi] + \mathcal{W}[\phi].$$

A computational example is provided in Fig. 3 (using the same numerics as in Fig. 3). A related, alternative version of a joint edge segmentation and registration functional uses one single edge set for both input images and thus does not require an explicit fitting term [19],

$$\tilde{\mathcal{J}}_{\text{edge}}[y_0, y_1, \mathcal{S}_{y_0}, \phi] = \mathcal{E}_{\text{MS}}^{\hat{y}_0}[y_0, \mathcal{S}_{y_0}] + \alpha \int_{\Omega} |y_1 - \hat{y}_1|^2 dx + a \int_{\Omega \setminus \phi^{-1}(\mathcal{S}_{y_0})} |\nabla y_1|^2 dx + \mathcal{W}[\phi].$$

#### 4. Phase field approximations of image segmentation and registration

The explicit treatment of sets such as image edges or homogeneous regions is difficult numerically for which reason phase field approximations of the Mumford–Shah functional have been developed. Those phase field approaches may also be adapted for joint image segmentation and registration.

The following paragraphs introduce the Modica–Mortola and the Ambrosio–Tortorelli functionals along with the corresponding functionals for joint segmentation and registration. Furthermore, Thms. 4.1 to 4.7 state the associated  $\Gamma$ -limits, the main results of this article.

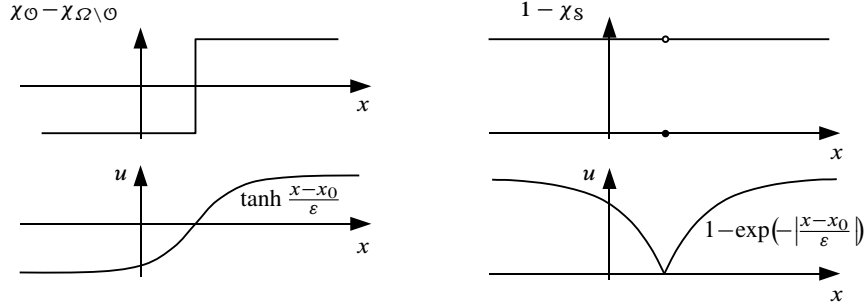


FIG. 4. 1D profiles of the optimal Modica–Mortola (bottom left, for  $\Psi(u) = (1 - u^2)^2$ ) and the Ambrosio–Tortorelli phase field (bottom right), approximating a piecewise constant function  $\chi_{\mathcal{O}} - \chi_{\Omega \setminus \mathcal{O}}$  and  $1 - \chi_S = 1 - \chi_{\{x_0\}}$ , respectively (where  $\chi$  denotes a characteristic function).

4.1 *Modica–Mortola model for region-based segmentation and registration*

The classical phase field approximation of the binary Mumford–Shah model is based on a Modica–Mortola-type double-well phase field  $u : \Omega \rightarrow \mathbb{R}$  [28]. The two disjoint segmentation regions are described by  $\{u \geq 0\}$  and  $\{u < 0\}$ , and the approximation of  $\mathcal{E}_{\text{bMS}}^{\hat{y}}$  is given by

$$\mathcal{E}_{\text{MM}}^{\hat{y}, \varepsilon}[(\underline{c}, \bar{c}), u] = \alpha \int_{\Omega} \frac{|1 + u|}{2} |\underline{c} - \hat{y}|^2 + \frac{|1 - u|}{2} |\bar{c} - \hat{y}|^2 dx + \nu \mathcal{L}_{\text{MM}}^{\varepsilon}[u],$$

where

$$\mathcal{L}_{\text{MM}}^{\varepsilon}[u] = \frac{1}{2} \int_{\Omega} \varepsilon |\nabla u|^2 + \frac{1}{\varepsilon} \Psi(u) dx.$$

Here,  $\Psi : \mathbb{R} \rightarrow \mathbb{R}$  denotes a potential with global minima  $\Psi(-1) = \Psi(1) = 0$  and  $\int_{-1}^1 \sqrt{\Psi(s)} ds = 1$ ,  $\Psi(s) \geq c(|s| - 1)$  for some  $c > 0$ . It is well-known that  $\mathcal{E}_{\text{MM}}^{\hat{y}, \varepsilon}$   $\Gamma$ -converges for  $\varepsilon \rightarrow 0$  against the binary Mumford–Shah segmentation functional with respect to the  $\mathbb{R}^2 \times L^1(\Omega)$ -topology,

$$\Gamma - \lim_{\varepsilon \rightarrow 0} \mathcal{E}_{\text{MM}}^{\hat{y}, \varepsilon} = \mathcal{E}_{\text{bMS}}^{\hat{y}} \quad \text{for}$$

$$\mathcal{E}_{\text{bMS}}^{\hat{y}}[(\underline{c}, \bar{c}), u] = \begin{cases} \mathcal{E}_{\text{bMS}}^{\hat{y}}[(\underline{c}, \bar{c}), \{u \geq 0\}] & \text{if } u \in \{-1, 1\} \text{ a. e.,} \\ \infty & \text{else,} \end{cases}$$

where we reused the symbol  $\mathcal{E}_{\text{bMS}}^{\hat{y}}$  with a little abuse of notation. In particular, the term  $\mathcal{L}_{\text{MM}}^{\varepsilon}$  converges against the perimeter of the segmented region and ensures that the phase field  $u$  takes values close to 1 or  $-1$  with a transition region of width  $\varepsilon$  between both regions  $\{u \approx 1\}$  and  $\{u \approx -1\}$  (Fig. 4, left). The term  $\mathcal{F}_{\text{vol}}[\mathcal{O}_0, \mathcal{O}_1, \phi]$  can be replaced using the mismatch penalty for the registration of two phase fields  $u_0, u_1$ ,

$$\mathcal{F}[u_0, u_1, \phi] = \int_{\Omega} (u_0 \circ \phi - u_1)^2 dx.$$

Hence, a phase field version of the functional  $\mathfrak{J}_{\text{vol}}$  from Sec. 3.1 reads

$$\begin{aligned} \mathfrak{J}_{\text{vol}}^\varepsilon[(\underline{c}_0, \bar{c}_0), (\underline{c}_1, \bar{c}_1), u_0, u_1, \phi] \\ = \mathfrak{E}_{\text{MM}}^{\hat{y}_0, \varepsilon}[(\underline{c}_0, \bar{c}_0), u_0] + \mathfrak{E}_{\text{MM}}^{\hat{y}_1, \varepsilon}[(\underline{c}_1, \bar{c}_1), u_1] + \frac{a}{4} \mathcal{F}[u_0, u_1, \phi] + \mathcal{W}[\phi]. \end{aligned}$$

This functional indeed  $\Gamma$ -converges against the expected sharp interface limit  $\mathfrak{J}_{\text{vol}}$ , so a coupling of Modica–Mortola phase fields with deformations is feasible.

**Theorem 4.1** ( $\Gamma$ -limit of joint region segmentation and matching) *With respect to convergence in  $\mathbb{R}^4 \times (L^1(\Omega))^2 \times w - W_{\text{id}}^{1,p}(\Omega)$  we have*

$$\begin{aligned} \Gamma - \lim_{\varepsilon \rightarrow 0} \mathfrak{J}_{\text{vol}}^\varepsilon &= \mathfrak{J}_{\text{vol}}^0 \quad \text{for} \\ \mathfrak{J}_{\text{vol}}^0[(\underline{c}_0, \bar{c}_0), (\underline{c}_1, \bar{c}_1), u_0, u_1, \phi] &= \mathfrak{J}_{\text{vol}}[(\underline{c}_0, \bar{c}_0), (\underline{c}_1, \bar{c}_1), \mathcal{O}_0, \mathcal{O}_1, \phi] \end{aligned}$$

if  $u_0, u_1 \in \{-1, 1\}$  a. e. and  $\infty$  else, where  $\mathcal{O}_i = \{u_i = 1\}$ .

**Remark 4.2** *The result and the proof can readily be adapted if the exponent 2 in the fitting term  $\mathcal{F}$  is replaced by any  $t \in (0, \infty)$ . Also, the terms of the form  $|c - \hat{y}|^2$  inside the Modica–Mortola segmentation may obviously be replaced by different types of indicators for the two image regions.*

#### 4.2 Ambrosio–Tortorelli model for edge-based segmentation and registration

The classical phase field approximation to the Mumford–Shah functional  $\mathfrak{E}_{\text{MS}}^{\hat{y}}$  is due to Ambrosio and Tortorelli [2] and encodes the edge set  $\mathcal{S}_y$  as the zero-level set of a single-well phase field  $u : \Omega \rightarrow \mathbb{R}$ ,

$$\mathfrak{E}_{\text{AT}}^{\hat{y}, \varepsilon}[y, u] = \int_{\Omega} (u^2 + k_\varepsilon) |\nabla y|^2 + \alpha |y - \hat{y}|^2 \, dx + \nu \mathfrak{L}_{\text{AT}}^\varepsilon[u],$$

where

$$\mathfrak{L}_{\text{AT}}^\varepsilon[u] = \frac{1}{2} \int_{\Omega} \varepsilon |\nabla u|^2 + \frac{1}{\varepsilon} (1 - u)^2 \, dx$$

and  $0 < k_\varepsilon = o(\varepsilon)$ . For  $\varepsilon \rightarrow 0$ ,  $\mathfrak{E}_{\text{AT}}^{\hat{y}, \varepsilon}$  indeed  $\Gamma$ -converges to  $\mathfrak{E}_{\text{MS}}^{\hat{y}}$  in the  $(L^1(\Omega))^2$ -topology [3],

$$\begin{aligned} \Gamma - \lim_{\varepsilon \rightarrow 0} \mathfrak{E}_{\text{AT}}^{\hat{y}, \varepsilon} &= \mathfrak{E}_{\text{MS}}^{\hat{y}} \quad \text{for} \\ \mathfrak{E}_{\text{MS}}^{\hat{y}}[y, u] &= \begin{cases} \mathfrak{E}_{\text{MS}}^{\hat{y}}[y, \mathcal{S}_y] & \text{if } u = 1 \text{ a. e.}, \\ \infty & \text{else,} \end{cases} \end{aligned}$$

where  $\mathcal{S}_y$  denotes the discontinuity set of  $y$  (with a little abuse of notation we reused the symbol  $\mathfrak{E}_{\text{MS}}^{\hat{y}}$ ). Here, too,  $\mathfrak{L}_{\text{AT}}^\varepsilon$  converges against the total length of the encoded edges and ensures that  $u$  takes approximately a  $1 - \exp(-|x|/\varepsilon)$  profile normal to the encoded edges (Fig. 4, right).

It turns out that the coupling of Ambrosio–Tortorelli phase fields with deformations produces several interesting effects that can most clearly be presented and understood in 1D, so  $\Omega$  will represent a real interval in the following. The subsequent theorems analyze several variants of joint

segmentation and registration functionals, thereby illustrating different phenomena. In each case, the matching term  $\mathfrak{F}_{\text{edge}}[\mathcal{S}_{y_0}, \mathcal{S}_{y_1}, \phi]$  is replaced by the phase field mismatch penalty  $\mathfrak{F}[u_0, u_1, \phi]$ , which has to be weighted with  $\frac{1}{\varepsilon}$  since the diffuse edges in  $u_0$  and  $u_1$  have width  $\sim \varepsilon$  (more precisely,  $\int_{-\infty}^{\infty} \exp(-2|x|/\varepsilon) = \varepsilon$ ), i.e.  $\frac{1}{\varepsilon} \mathfrak{F}[u_0, u_1, \phi]$  should scale like  $\mathfrak{F}_{\text{edge}}[\mathcal{S}_{y_0}, \mathcal{S}_{y_1}, \phi]$ .

**4.2.1 Consecutive edge segmentation and registration.** We first consider the case of non-simultaneous, consecutive segmentation and edge registration, in which already the first difference to the volume matching case can be observed: While the fitting term is actually intended to measure the symmetric difference between both image edge sets, only an asymmetric, one-directional mismatch penalty survives in the  $\Gamma$ -limit.

Denote the set of minimizers of  $\mathfrak{E}_{\text{AT}}^{\hat{y}, \varepsilon}$  by  $\mathfrak{m}^\varepsilon(\hat{y}) \subset W^{1,2}(\Omega) \times W^{1,2}(\Omega)$ . Likewise, let us define  $\mathfrak{m}^0(\hat{y}) \subset \text{pw-}W^{1,2}(\Omega)$  to be that subset of the minimizers of  $\mathfrak{E}_{\text{MS}}^{\hat{y}}$  such that each element  $y \in \mathfrak{m}^0(\hat{y})$  is the  $L^1(\Omega)$ -limit of a sequence  $y^j$  with  $y^j \in \mathfrak{m}^{\varepsilon_j}(\hat{y})$  for some sequence  $\varepsilon_j \rightarrow 0$  (note that a minimizing pair  $(y, \mathcal{S}_y)$  of  $\mathfrak{E}_{\text{MS}}^{\hat{y}}$  is already uniquely defined by its first component,  $y$ ). The functional

$$\mathfrak{J}^\varepsilon[\phi] = \inf_{\substack{(y_0, u_0) \in \mathfrak{m}^\varepsilon(\hat{y}_0) \\ (y_1, u_1) \in \mathfrak{m}^\varepsilon(\hat{y}_1)}} \frac{a}{\varepsilon} \mathfrak{F}[u_0, u_1, \phi] + \mathcal{W}[\phi]$$

now serves for the registration of the Ambrosio–Tortorelli phase fields belonging to the input images  $\hat{y}_0, \hat{y}_1$ .

**Theorem 4.3** ( $\Gamma$ -limit of consecutive edge segmentation and matching) *In 1D and with respect to weak convergence in  $W_{\text{id}}^{1,p}(\Omega)$  we have*

$$\Gamma - \lim_{\varepsilon \rightarrow 0} \mathfrak{J}^\varepsilon = \mathfrak{J}^0 \quad \text{for}$$

$$\mathfrak{J}^0[\phi] = \inf_{\substack{y_0 \in \mathfrak{m}^0(\hat{y}_0) \\ y_1 \in \mathfrak{m}^0(\hat{y}_1)}} a \mathcal{H}^0(\mathcal{S}_{y_1} \setminus \phi^{-1}(\mathcal{S}_{y_0})) + \mathcal{W}[\phi],$$

where  $\mathcal{S}_y$  denotes the jump set of an image  $y \in \text{pw-}W^{1,2}(\Omega)$ .

The reason for the asymmetric matching term in the limit is that the matching deformation  $\phi$  can squeeze the phase field  $u_0$  in such a way that  $u_0 \circ \phi$  encodes fewer edges than  $u_0$ . Fig. 5 illustrates this phenomenon for a fixed  $\varepsilon > 0$ . The smaller  $\varepsilon$ , the stronger the phase field is squeezed, and in the limit  $\varepsilon \rightarrow 0$  an edge can vanish completely. Note that this can happen despite the control on the Jacobian determinant of the deformation in  $\mathcal{W}$ , since the required blow-up of the determinant is confined to an arbitrarily small set as  $\varepsilon \rightarrow 0$ .

**Remark 4.4** *By inspection of the proof, a possibility to also enforce penalization of  $\phi^{-1}(\mathcal{S}_{y_0}) \not\subset \mathcal{S}_{y_1}$  consists in weighting the mismatch term with  $\frac{1}{\varepsilon^t}$  instead of  $\frac{1}{\varepsilon}$  for some  $t > 1 + \frac{1}{p}$  (where  $p$  is the exponent from condition 5 on the hyperelastic energy density). However, the mismatch penalty then turns into a strict constraint: The  $\Gamma$ -limit will only be finite for  $\phi^{-1}(\mathcal{S}_{y_0}) = \mathcal{S}_{y_1}$ .*

**4.2.2 Joint edge segmentation and registration.** For the purpose of simultaneous edge segmentation and registration, the phase field version of the functional  $\mathfrak{J}_{\text{edge}}$  from Sec. 3.2 reads

$$\mathfrak{J}_{\text{edge}}^\varepsilon[y_0, y_1, u_0, u_1, \phi] = \mathfrak{E}_{\text{AT}}^{\hat{y}_0, \varepsilon}[y_0, u_0] + \mathfrak{E}_{\text{AT}}^{\hat{y}_1, \varepsilon}[y_1, u_1] + \frac{a}{\varepsilon} \mathfrak{F}[u_0, u_1, \phi] + \mathcal{W}[\phi].$$

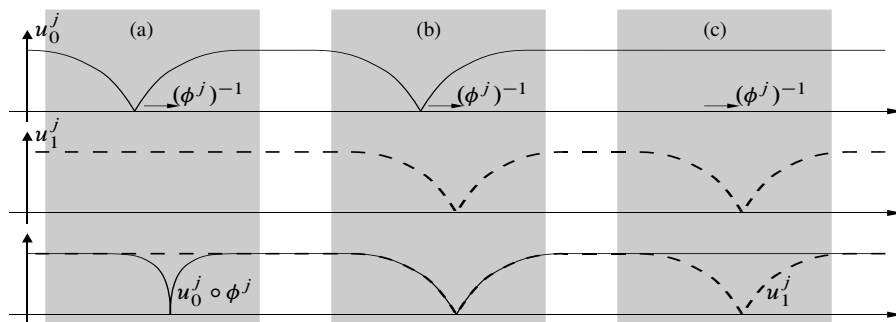


FIG. 5. Schematic diagram of the recovery sequence for Thm. 4.3. From a sequence  $\varepsilon_j \rightarrow 0$  we pick one element and show the corresponding approximations  $\phi^j$  and  $(y_i^j, u_i^j) \in m^{\varepsilon_j}(\hat{y}_i)$ ,  $i = 0, 1$ , to a given deformation  $\phi$  and  $(y_i, u_i) \in m^0(\hat{y}_i)$  (in this sketch,  $\phi$  is a simple translation).  $\phi^j$  squeezes  $u_0^j$  around points in  $\phi^{-1}(\mathcal{S}_{y_0}) \setminus \mathcal{S}_{y_1}$  (case (a)) and maintains the optimal profile (neither dilates nor compresses) around points in  $\phi^{-1}(\mathcal{S}_{y_0}) \cup \mathcal{S}_{y_1}$  ((b) and (c)).

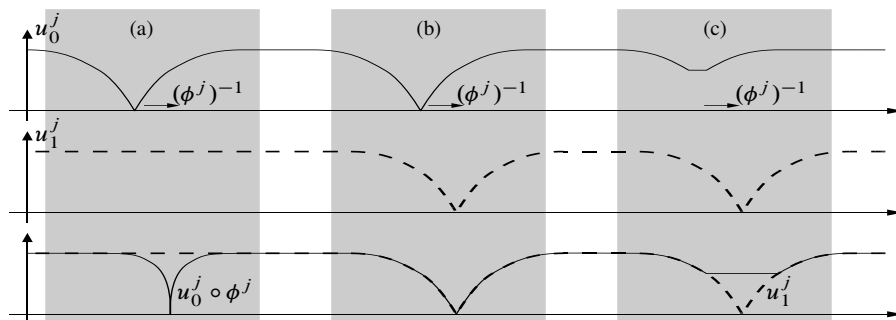


FIG. 6. Schematic diagram of the recovery sequence for Thm. 4.5. As in Fig. 5 we show for a fixed  $\varepsilon_j$  the approximations  $\phi^j$  and  $u_0^j, u_1^j$  to a given deformation  $\phi$  and phase fields  $u_0, u_1$  (in this sketch,  $\phi$  is a simple translation). In addition to the squeezing effect from Fig. 5,  $u_0^j$  has developed ghost edges around  $\phi(\mathcal{S}_{y_1}) \setminus \mathcal{S}_{y_0}$  which are further diluted by  $\phi^j$  (case (c)).

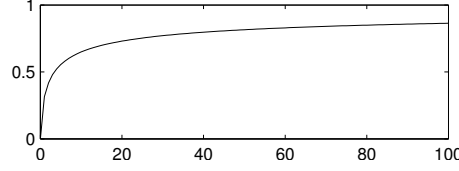
Here again the edges in the phase field  $u_0$  get squeezed where  $u_1$  has no edge. In addition, a new effect occurs: In order to reduce the fitting term  $\frac{a}{\varepsilon} \mathcal{F}[u_0, u_1, \phi]$ , spurious ghost edges appear in the phase field  $u_0$  at places where  $u_1$  exhibits an edge (Fig. 6). As a result, not only is the mismatch penalty asymmetric, but also its weight is bounded above in the limit.

**Theorem 4.5** ( $\Gamma$ -limit of joint edge segmentation and matching) *In 1D and with respect to convergence in  $(L^1(\Omega))^4 \times w - W_{\text{id}}^{1,p}(\Omega)$  we have*

$$\Gamma - \lim_{\varepsilon \rightarrow 0} \mathfrak{G}_{\text{edge}}^\varepsilon = \mathfrak{G}_{\text{edge}}^0 \quad \text{for}$$

$$\mathfrak{G}_{\text{edge}}^0[y_0, y_1, u_0, u_1, \phi] = \mathfrak{E}_{\text{MS}}^{y_0}[y_0, u_0] + \mathfrak{E}_{\text{MS}}^{y_1}[y_1, u_1] + \nu Z^{0,1}\left(\frac{a}{\nu}\right) \mathcal{H}^0(\phi(\mathcal{S}_{y_1}) \setminus \mathcal{S}_{y_0}) + \mathcal{W}[\phi],$$

where  $Z^{0,1}(a) = \min_{l \in [0,1]} (2 \int_0^l \sqrt{(1-z)^2 + 2a(l-z)^2} dz + 4 \int_l^1 \sqrt{(1-z)^2} dz) - 1$  is a monotonous and concave function with  $Z^{0,1}(0) = 0$ ,  $(Z^{0,1})'(0) = 1$ , and  $\lim_{a \rightarrow \infty} Z^{0,1}(a) = 1$  (Fig. 7).

FIG. 7. The function  $Z^{0,1} : [0, \infty) \rightarrow [0, 1]$ 

The ghost edges are actually not so much of a surprise. In fact, they are expected and even desired to segment an input image with very weak edges based on the edges from the other input image (indeed, this is the benefit from joint segmentation and registration, cf. Fig. 1). The ghost edges are the more pronounced the higher the matching weight  $a$  is.

The function  $Z^{0,1}$  expresses the balance between the fitting term  $\frac{a}{\varepsilon} \mathcal{F}[u_0, u_1, \phi]$  and the penalization  $\nu \mathcal{L}_{\text{AT}}^\varepsilon[u_0]$  of ghost edges. For small weight  $a$  it is cheaper to allow a mismatch between both phase fields, while for large  $a$  it is better to reduce the fitting term via developing a ghost edge (which is only penalized with weight  $\nu$ ). As a result, the weight of the mismatch penalty in the limit is always smaller than  $\min(a, \nu)$ .

While the mismatch penalty weight cannot be increased in the limit, a remedy for the asymmetric matching can be obtained by scaling the term  $\mathcal{F}[u_0, u_1, \phi]$  differently,

$$\mathfrak{J}_{\text{edge}}^{t,\varepsilon}[y_0, y_1, u_0, u_1, \phi] = \mathcal{E}_{\text{AT}}^{\hat{y}_0,\varepsilon}[y_0, u_0] + \mathcal{E}_{\text{AT}}^{\hat{y}_1,\varepsilon}[y_1, u_1] + \frac{a}{\varepsilon^t} \mathcal{F}[u_0, u_1, \phi] + \mathcal{W}[\phi].$$

If for  $\varepsilon \rightarrow 0$  the weight of  $\mathcal{F}[u_0, u_1, \phi]$  tends to infinity fast enough, then the squeezing mechanism from Fig. 6 no longer suffices to annihilate the mismatch penalty, and both  $u_0$  and  $u_1$  are forced to form fully developed ghost edge profiles.

**Theorem 4.6** (Symmetric  $\Gamma$ -limit of joint edge segmentation and matching) *Let  $t \in (1, \frac{r}{r-1}) \cup (\frac{p}{p-1}, \infty)$ , where  $p$  and  $r$  are the exponents from conditions 5 and 6 on the hyperelastic energy density. In 1D and with respect to convergence in  $(L^1(\Omega))^4 \times w - W_{\text{id}}^{1,p}(\Omega)$  we have*

$$\Gamma - \lim_{\varepsilon \rightarrow 0} \mathfrak{J}_{\text{edge}}^{t,\varepsilon} = \mathfrak{J}_{\text{edge}}^{t,0} \quad \text{for}$$

$$\mathfrak{J}_{\text{edge}}^{t,0}[y_0, y_1, u_0, u_1, \phi] = \mathcal{E}_{\text{MS}}^{\hat{y}_0}[y_0, u_0] + \mathcal{E}_{\text{MS}}^{\hat{y}_1}[y_1, u_1] + \nu \mathcal{F}_{\text{edge}}[S_{y_0}, S_{y_1}, \phi] + \mathcal{W}[\phi]$$

if  $t > \frac{p}{p-1}$  and otherwise

$$\mathfrak{J}_{\text{edge}}^{t,0}[y_0, y_1, u_0, u_1, \phi] = \mathcal{E}_{\text{MS}}^{\hat{y}_0}[y_0, u_0] + \mathcal{E}_{\text{MS}}^{\hat{y}_1}[y_1, u_1] + \nu \mathcal{H}^0(\phi(S_{y_1}) \setminus S_{y_0}) + \mathcal{W}[\phi].$$

**4.2.3 Joint segmentation and edge to image registration.** As a final example for joint segmentation and registration using Ambrosio–Tortorelli phase fields we consider the functional employed in [21, 23],

$$\tilde{\mathfrak{J}}_{\text{edge}}^\varepsilon[y_0, y_1, u_0, \phi] = \mathcal{E}_{\text{AT}}^{\hat{y}_0,\varepsilon}[y_0, u_0] + \alpha \int_{\Omega} |y_1 - \hat{y}_1|^2 dx + a \int_{\Omega} ((u_0 \circ \phi)^2 + k_\varepsilon) |\nabla y_1|^2 dx + \mathcal{W}[\phi],$$

which only uses one single edge phase field for both images and thus represents a phase field version of the functional  $\tilde{\mathfrak{J}}_{\text{edge}}$  from Sec. 3.2.

**Theorem 4.7** ( $\Gamma$ -limit of joint segmentation and edge to image matching) *In 1D and with respect to convergence in  $(L^1(\Omega))^3 \times w - W_{\text{id}}^{1,p}(\Omega)$  we have*

$$\Gamma - \lim_{\varepsilon \rightarrow 0} \tilde{\mathcal{J}}_{\text{edge}}^\varepsilon = \tilde{\mathcal{J}}_{\text{edge}}^0 \quad \text{for}$$

$$\tilde{\mathcal{J}}_{\text{edge}}^0[y_0, y_1, u_0, \phi] = \mathcal{E}_{\text{MS}}^{\hat{y}_0}[y_0, u_0] + \alpha \int_{\Omega} |y_1 - \hat{y}_1|^2 dx + a \int_{\Omega \setminus \mathcal{S}_{y_1}} |\nabla y_1|^2 dx + \nu \mathcal{H}^0(\phi(\mathcal{S}_{y_1}) \setminus \mathcal{S}_{y_0}) + \mathcal{W}[\phi].$$

Obviously, this model exhibits the same properties as the previous ones, i.e. the mismatch penalty in the limit is asymmetric, and its weight equals the weight of the length regularization inside the segmentation.

**4.2.4 Joint edge segmentation and registration in higher dimensions.** The previous paragraphs have shown that – without additional symmetrization – simultaneous Ambrosio–Tortorelli segmentation and registration of the edge phase fields in 1D generally results in an asymmetric, partial mismatch penalty in the  $\Gamma$ -limit. In higher dimensions, the situation becomes worse: It may happen that the registration fails to couple the segmentation of both images, also neglecting the mismatch  $\phi(\mathcal{S}_{y_1}) \setminus \mathcal{S}_{y_0}$  and thus leading to two completely independent segmentation problems without any mismatch penalty. The following example uses the functional  $\mathcal{J}_{\text{edge}}^\varepsilon$  from Sec. 4.2.2.

**Example 4.8** (A disturbing example) *Let  $\Omega = (-1, 1)^2$ , and let  $W(A) = \|A\|_F^p + \det A^r + \det A^{-s} - 2 - 2^{p/2}$  for  $A \in \mathbb{R}^{2 \times 2}$  with  $\det A \geq 0$ , where the parameters and exponents are chosen to satisfy conditions 1 to 6 on the hyperelastic energy density. Furthermore, define  $\hat{y}_0, \hat{y}_1, y_0, y_1, u_0, u_1 : \Omega \rightarrow \mathbb{R}, \phi : \Omega \rightarrow \Omega$  as  $\phi \equiv \text{id}, u_0 \equiv u_1 \equiv 1, \hat{y}_0 \equiv y_0 \equiv 0$ , and  $\hat{y}_1(x_1, x_2) = y_1(x_1, x_2) = \text{sgn}(x_1)$ . Then with respect to convergence in  $(L^1(\Omega))^4 \times w - W_{\text{id}}^{1,p}(\Omega)$  we have*

$$(\Gamma - \lim_{\varepsilon \rightarrow 0} \mathcal{J}_{\text{edge}}^\varepsilon)[y_0, y_1, u_0, u_1, \phi] = \mathcal{J}_{\text{edge}}^{0,2D}[y_0, y_1, u_0, u_1, \phi] \quad \text{for}$$

$$\mathcal{J}_{\text{edge}}^{0,2D}[y_0, y_1, u_0, u_1, \phi] = \mathcal{E}_{\text{MS}}^{\hat{y}_0}[y_0, u_0] + \mathcal{E}_{\text{MS}}^{\hat{y}_1}[y_1, u_1] + \mathcal{W}[\phi].$$

The above  $\Gamma$ -convergence of  $\mathcal{J}_{\text{edge}}^\varepsilon$  to  $\mathcal{J}_{\text{edge}}^{0,2D}$  is expected to hold generally in higher dimensions, but a proof in the case of a non-smooth matching deformation  $\phi$  is still pending. The underlying observation is the following: Wherever the image  $\hat{y}_0$  exhibits an edge which  $\hat{y}_1$  does not have, the squeezing mechanism from Figs. 5 and 6 eliminates the mismatch penalty. Wherever  $\hat{y}_1$  has an edge but  $\hat{y}_0$  does not, the phase field  $u_0$  will develop a sequence of short ghost edge profiles which are separated by larger intermediate spaces (Fig. 8). Since the ghost edge segments are short, they do not add much to the length penalization  $\nu \mathcal{L}_{\text{AT}}^\varepsilon[u_0]$ . Furthermore, in the pullback  $u_0 \circ \phi$  these segments are elongated so that they almost generate a continuous ghost edge and the mismatch penalty gets small. If for  $\varepsilon \rightarrow 0$  the length of the ghost edge segments goes to zero faster than the length of the intermediate spaces, then in the limit both  $\frac{a}{\varepsilon} \mathcal{F}[u_0, u_1, \phi]$  and  $\nu \mathcal{L}_{\text{AT}}^\varepsilon[u_0]$  disappear. Also, the deformation  $\phi$  only exhibits strong deformations and compressions in the immediate proximity of the diffuse ghost edges so that the required additional deformation energy is small and vanishes in the limit.

**Remark 4.9** *The decoupling of both segmentation problems does not only occur for the joint segmentation and registration functional from Sec. 4.2.2. By a similar construction as in the proof of*

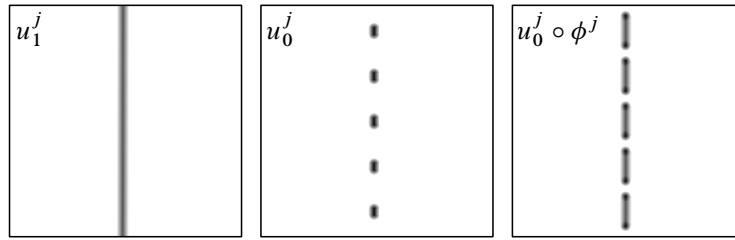


FIG. 8. Schematic diagram of the recovery sequence for Ex. 4.8. As in Fig. 6 we show for a fixed  $\varepsilon_j$  the approximations  $u_0^j, u_1^j$ , and  $u_0^j \circ \phi^j$  to given  $u_0, u_1$ , and  $u_0 \circ \phi$ .  $u_1^j$  develops a full vertical edge, since the original image  $\hat{y}_1$  exhibits a vertical discontinuity.  $u_0^j$  develops a sequence of short diffuse ghost edge segments which are elongated in the pullback  $u_0^j \circ \phi^j$ .

the above example one observes that the mismatch term also vanishes in the limit for the functional from Sec. 4.2.3.

4.2.5 *Appropriate functional modifications.* In summary, the introduced functionals for joint Ambrosio–Tortorelli edge segmentation and registration exhibit the following deficiencies in the limit  $\varepsilon \rightarrow 0$ .

- Instead of penalizing the symmetric difference  $\mathcal{S}_{y_1} \Delta \phi^{-1}(\mathcal{S}_{y_0})$ , the  $\Gamma$ -limit ignores all edges in  $\phi^{-1}(\mathcal{S}_{y_0}) \setminus \mathcal{S}_{y_1}$  (Thms. 4.3, 4.5, and 4.7). This is caused by the deformation  $\phi$  squeezing the phase field profile of  $u_0$  such that in the limit, edges in  $u_0 \circ \phi$  can become invisible.
- In 1D, the penalty weight  $a$  of the mismatch is strongly reduced and in fact can never exceed the length parameter  $\nu$  (Thms. 4.5, 4.6, and 4.7). This effect is produced by spurious diffuse ghost edges that occur in phase field  $u_0$  in order to make  $u_0 \circ \phi$  look more like  $u_1$ .
- In higher dimensions, the mismatch penalty vanishes completely (Ex. 4.8). Again, this is due to ghost edges in  $u_0 \circ \phi$ , but the mechanism of their emergence differs from 1D: Diffuse ghost edges form from small, very localized seeds in  $u_0$  which are dilated by the deformation to fully developed diffuse edges in  $u_0 \circ \phi$ .

Obviously, the reason why these functionals work satisfactorily in practice (as in Figs. 1 and 3) must be the use of an  $\varepsilon$  away from zero. We now briefly discuss the phenomena, including suggestions for improvements of the joint segmentation and registration functionals.

The second effect described above is what distinguishes joint edge segmentation and registration from the consecutive approach (cf. Thms. 4.3 and 4.5). In fact, this property is not a deficiency of the Ambrosio–Tortorelli phase field approximation, but already holds for the sharp interface energy. Indeed, the sharp interface functional  $\mathfrak{J}_{\text{edge}}$  is not well-posed for  $a > \nu$ , since then both  $y_0$  and  $y_1$  could develop a tiny edge in all places where the respective other image has one, thereby making the fitting term  $\mathfrak{F}_{\text{edge}}$  vanish and only adding the edge length weighted by  $\nu$ . The well-posed relaxation of that functional would have weight  $a$  replaced by  $\nu$ . Effectively, this effect represents one of the strengths of joint segmentation and registration: Edges which are too weak in one image can still be segmented based on the edge information in the other image, which is made available by the registration. The weight  $\nu$  should be chosen so large that segmentation of irrelevant edges is suppressed; this weight will then also be appropriate for the matching of the edges.

As for the first effect, the edge squeezing, an obvious remedy is to consider a more symmetric matching term of the form  $\frac{a}{\varepsilon}(\mathfrak{F}[u_0, u_1, \phi] + \mathfrak{F}[u_1, u_0, \phi^{-1}])$ . However, this modification is

most probably still too weak to avoid the third above-listed mechanism that occurs in higher dimensions. To do away with both effects, one can replace the deformation energy  $\mathcal{W}[\phi]$  by  $\mathcal{W}[\phi] + \int_{\Omega} |\mathfrak{D}^2\phi|^p dx$ . The  $\Gamma$ -limit would then naturally be considered with respect to weak convergence of deformations in  $W^{2,p}(\Omega)$ . If  $p > d$ , any weakly converging sequence of deformations  $\phi$  with bounded energy would be uniformly bounded in  $C^1(\Omega)$  so that a complete squeezing of edges or a dilation of ghost edge segments can no longer occur and thus the  $\Gamma$ -limit retains a term penalizing the mismatch between the edge sets. Note though that the edge phase fields can still be squeezed or dilated by a finite amount so that the weight of the mismatch term will depend on the elastic energy density  $W$  and the limit deformation  $\phi$ . A few additional comments in this direction are provided later in Sec. 5.6.

Finally, Remark 4.4 and Thm. 4.6 already suggest an alternative remedy: One could increase the rate at which the weight of the mismatch term tends to infinity as  $\varepsilon \rightarrow 0$ . For a sufficiently large rate, the mismatch term would begin to cost too much for edges that occur in  $\mathfrak{S}_{y_1}$  but not in  $\mathfrak{S}_{y_0}$ , despite oscillating deformations as in Fig. 8. Therefore  $u_0$  will develop a full ghost phase field, resulting in the mismatch penalty  $\nu \mathcal{H}^{d-1}(\phi(\mathfrak{S}_{y_1}) \setminus \mathfrak{S}_{y_0})$ . We may conjecture that for the functional  $\mathfrak{J}_{\text{edge}}^{t,\varepsilon}$  from Sec. 4.2.2 and for any dimension  $d$  there exists indeed a  $t$  large enough such that

$$\Gamma - \lim_{\varepsilon \rightarrow 0} \mathfrak{J}_{\text{edge}}^{t,\varepsilon} = \mathfrak{J}_{\text{edge}}^{t,0} \quad \text{with}$$

$$\mathfrak{J}_{\text{edge}}^{t,0}[y_0, y_1, u_0, u_1, \phi]$$

$$= \mathfrak{E}_{\text{MS}}^{y_0}[y_0, u_0] + \mathfrak{E}_{\text{MS}}^{y_1}[y_1, u_1] + \nu \mathcal{H}^{d-1}\left(\left(\phi^{-1}(\mathfrak{S}_{y_0}) \setminus \mathfrak{S}_{y_1}\right) \cup \left(\phi(\mathfrak{S}_{y_1}) \setminus \mathfrak{S}_{y_0}\right)\right) + \mathcal{W}[\phi].$$

This would represent a satisfactory result since  $\mathfrak{J}_{\text{edge}}^{t,\varepsilon}$  approximates a functional that penalizes a bad registration via a mismatch of edges and at the same time reconstructs edges based on information from both input images. For practical purposes this would just imply that for a fixed chosen phase field parameter one would have to choose a sufficiently large weight of the mismatch term. The analysis of this limit problem promises to be much more involved than the 1D problems considered here. In particular, as yet it is unclear how to treat the coupling of non-smooth deformations with curved edge phase fields, a problem to be examined in future work.

## 5. Proofs

The following sections are devoted to the proofs of the  $\Gamma$ -convergence results from the previous section. Furthermore, in Sec. 5.6 we include a brief discussion on the influence of tangential deformations in edge-based segmentation and registration in higher dimensions.

### 5.1 Proof of Theorem 4.1

The treatment of all energy terms is standard except for the matching term  $\mathfrak{F}$ , whose sequential lower semi-continuity represents the only technical difficulty and follows from the subsequent lemma.

**Lemma 5.1** *Let  $u^j \rightarrow u$  in  $L^1(\Omega)$  as  $j \rightarrow \infty$ , where  $u \in \text{BV}(\Omega)$  is a function of bounded variation taking only values  $-1$  and  $1$ . Further let  $\phi^j \rightarrow \phi$  in  $W_{\text{id}}^{1,p}(\Omega)$  as  $j \rightarrow \infty$  such that  $\mathcal{W}[\phi^j]$  is uniformly bounded. Then  $u^j \circ \phi^j \rightarrow u \circ \phi$  in  $L^1(\Omega)$ .*

*Proof.* Let  $\mathcal{O} = \{x \in \Omega : u(x) = 1\}$ . We show  $u^j \circ \phi^j \rightarrow u \circ \phi$  in  $L^1(\phi^{-1}(\mathcal{O}))$ ; the convergence in  $L^1(\phi^{-1}(\Omega \setminus \mathcal{O}))$  can be shown analogously.

First note that, due to the conditions on  $\mathcal{W}$  in Sec. 2,  $\mathcal{W}[\phi]$  is bounded and the  $\phi^j$  and  $\phi$  are homeomorphisms with  $\det \mathfrak{D}\phi^j, \det \mathfrak{D}\phi > 0$  almost everywhere. Furthermore,  $\phi^j \rightarrow \phi$  in  $C^{0,\omega}(\bar{\Omega})$  for any  $\omega < 1 - \frac{d}{p}$  due to the compact embedding  $W^{1,p}(\Omega) \subset C^{0,\omega}(\bar{\Omega})$ . Finally, by the calculation in Sec. 2 we have

$$\|(\phi^j)^{-1}\|_{W^{1,\tilde{q}}(\Omega)}^{\tilde{q}} = \int_{\Omega} \|(\mathfrak{D}\phi^j)^{-1}\|_F^{\tilde{q}} \det \mathfrak{D}\phi^j \, dx \leq \frac{1}{C_1} (\mathcal{W}[\phi^j] + C_2|\Omega|)^{\frac{\tilde{q}}{q}} (\mathcal{W}[\phi] + C_2|\Omega|)^{\frac{q-\tilde{q}}{q}}$$

so that any subsequence of  $(\phi^j)^{-1}$  admits a weakly converging subsequence in  $W^{1,\tilde{q}}(\Omega)$  and by compact embedding a strongly converging subsequence in  $C^{0,\tilde{\omega}}(\bar{\Omega})$  for any  $\tilde{\omega} < 1 - \frac{d}{\tilde{q}}$ . The limit for any such subsequence must necessarily be  $\phi^{-1}$  so that altogether  $(\phi^j)^{-1} \rightarrow \phi^{-1}$  in  $C^{0,\tilde{\omega}}(\bar{\Omega})$ . Now for any measurable set  $S \subset \Omega$  with Lebesgue measure  $\text{vol}(S) \leq \eta$  we have  $\text{vol}(\phi^{-1}(S)) \leq C \eta^{\frac{s}{1+s}}$  and  $\text{vol}(\phi^j(S)) \leq C \eta^{1-\frac{d}{p}}$  for some constant  $C$  and the exponents  $p, s$  from condition 5 on the energy density  $W$ . Indeed,

$$\begin{aligned} \int_{\phi^{-1}(S)} dx &= \int_S \frac{1}{\det \mathfrak{D}\phi \circ \phi^{-1}} dx \leq \left( \int_S dx \right)^{\frac{s}{1+s}} \left( \int_S \left( \frac{1}{\det \mathfrak{D}\phi \circ \phi^{-1}} \right)^{1+s} dx \right)^{\frac{1}{1+s}} \\ &\leq \eta^{\frac{s}{1+s}} \left( \int_{\Omega} (\det \mathfrak{D}\phi)^{-s} dx \right)^{\frac{1}{1+s}} \leq (\mathcal{W}[\phi])^{\frac{1}{1+s}} \eta^{\frac{s}{1+s}}, \end{aligned}$$

where we have exploited the bijectivity of  $\phi : \Omega \rightarrow \Omega$  and the corresponding change of variables, the boundedness of  $\mathcal{W}[\phi]$ , and Hölder's inequality. Likewise,

$$\begin{aligned} \int_{\phi^j(S)} dx &= \int_S \det \mathfrak{D}\phi^j \, dx \leq d! \int_S \|\mathfrak{D}\phi^j\|_F^d dx \\ &\leq d! \left( \int_S dx \right)^{1-\frac{d}{p}} \left( \int_S \|\mathfrak{D}\phi^j\|_F^p dx \right)^{\frac{d}{p}} \leq d! (\mathcal{W}[\phi^j])^{\frac{d}{p}} \eta^{1-\frac{d}{p}}. \end{aligned}$$

Now, for any  $h > 0$  we can find an open set  $E_h \subset \Omega$  with smooth boundary such that  $\text{vol}(E_h \Delta \mathcal{O}) \leq h$  [1, Thm. 3.42], [8, Prop. A.17]. Hence,

$$\begin{aligned} &\text{vol}(\phi^j(\phi^{-1}(\mathcal{O}))\Delta\mathcal{O}) \\ &\leq \text{vol}(\phi^j(\phi^{-1}(\mathcal{O}\Delta E_h))) + \text{vol}(\phi^j(\phi^{-1}(E_h))\Delta E_h) + \text{vol}(E_h\Delta\mathcal{O}) \rightarrow h^{(1-\frac{d}{p})\frac{s}{1+s}} + h \end{aligned}$$

for  $j \rightarrow \infty$ .<sup>1</sup> By the arbitrariness of  $h$ ,  $\text{vol}(\phi^j(\phi^{-1}(\mathcal{O}))\Delta\mathcal{O}) \rightarrow 0$ .

Given  $\eta > 0$ , by Egorov's theorem there is a set  $S_\eta$  with Lebesgue measure  $\text{vol}(S_\eta) < \eta$  such that  $u^j \rightarrow u$  uniformly on  $\Omega \setminus S_\eta$ . Now choose  $k \in \mathbb{N}$  large enough so that for all  $j \geq k$  we have

<sup>1</sup> Note that  $\phi^j \circ \phi^{-1} \rightarrow \text{id}$  in some Hölder space (cf. Sec. 2), and thus the Hausdorff distance  $d_j$  between the compact sets  $\bar{E}_h$  and  $\phi^j \circ \phi^{-1}(\bar{E}_h)$  converges to zero. Then, however, due to  $\phi^j \circ \phi^{-1}(E_h) \subset \phi^j \circ \phi^{-1}(\bar{E}_h) \subset B_{d_j}(E_h)$  we have  $\text{vol}(\phi^j \circ \phi^{-1}(E_h)\Delta E_h) \leq \text{vol}(B_{d_j}(E_h) \setminus E_h) \leq d_j \kappa \mathcal{H}^{d-1}(\partial E_h)$ , where the constant  $\kappa$  depends on the maximum mean curvature of  $\partial E_h$ .

$\text{vol}(\phi^j(\phi^{-1}(\mathcal{O}))\Delta\mathcal{O}) < \eta$  and  $u^j|_{\mathcal{O}\setminus S_\eta} \geq 1 - \eta$ . Then

$$\begin{aligned} \|u^j \circ \phi^j - u \circ \phi\|_{L^1(\phi^{-1}(\mathcal{O}))} &= \int_{\phi^{-1}(\mathcal{O})} |u^j \circ \phi^j - 1| \, dx \\ &= \int_{\phi^j(\phi^{-1}(\mathcal{O}))} |u^j - 1| \frac{1}{\det \mathfrak{D}\phi^j \circ (\phi^j)^{-1}} \, dx \\ &\leq \int_{\mathcal{O}\setminus S_\eta} \frac{\eta}{\det \mathfrak{D}\phi^j \circ (\phi^j)^{-1}} \, dx \\ &\quad + \int_{S_\eta} \frac{2}{\det \mathfrak{D}\phi^j \circ (\phi^j)^{-1}} \, dx \\ &\quad + \int_{\phi^j(\phi^{-1}(\mathcal{O}))\Delta\mathcal{O}} \frac{2}{\det \mathfrak{D}\phi^j \circ (\phi^j)^{-1}} \, dx. \end{aligned}$$

These three terms scale like a positive power of  $\eta$  and can thus be made arbitrarily small, which was to be shown.  $\square$

The  $\Gamma$ -convergence result now is straightforward.

*Proof of Thm. 4.1.* First note that for  $\hat{y} \in L^\infty(\Omega)$  the energy

$$[(\underline{c}, \bar{c}), u] \mapsto \int_{\Omega} \frac{|1+u|}{2} |\underline{c} - \hat{y}|^2 + \frac{|1-u|}{2} |\bar{c} - \hat{y}|^2 \, dx$$

is (sequentially) continuous in  $\mathbb{R}^2 \times L^1(\Omega)$ . As a consequence, both terms of the above form may be neglected during the following  $\Gamma$ -convergence analysis.

For the lim sup-inequality we require a recovery sequence. Assume  $\underline{c}_0, \bar{c}_0, \underline{c}_1, \bar{c}_1, u_0, u_1, \phi$  to be given with  $\mathfrak{I}_{\text{vol}}^0[(\underline{c}_0, \bar{c}_0), (\underline{c}_1, \bar{c}_1), u_0, u_1, \phi] < \infty$ . Let  $u_0^\varepsilon, u_1^\varepsilon : \Omega \rightarrow [-1, 1]$  with  $u_0^\varepsilon \rightarrow u_0, u_1^\varepsilon \rightarrow u_1$  in  $L^1(\Omega)$  be standard recovery sequences for the  $\Gamma$ -convergence of  $\mathfrak{L}_{\text{MM}}^\varepsilon$  [28], [8, proof of Thm. 6.4], and define the recovery sequences for  $\underline{c}_0, \bar{c}_0, \underline{c}_1, \bar{c}_1, \phi$  to be the constant sequences. Then the convergence of all terms in  $\mathfrak{I}_{\text{vol}}^\varepsilon[(\underline{c}_0^\varepsilon, \bar{c}_0^\varepsilon), (\underline{c}_1^\varepsilon, \bar{c}_1^\varepsilon), u_0^\varepsilon, u_1^\varepsilon, \phi^\varepsilon]$  against the corresponding terms in  $\mathfrak{I}_{\text{vol}}^0[(\underline{c}_0, \bar{c}_0), (\underline{c}_1, \bar{c}_1), u_0, u_1, \phi]$  is obvious except for the matching term. However,  $\int_{\Omega} |u_0^\varepsilon \circ \phi^\varepsilon - u_1^\varepsilon|^2 \, dx \rightarrow_{\varepsilon \rightarrow 0} \int_{\Omega} |u_0 \circ \phi - u_1|^2 \, dx$  follows immediately by Lebesgue's convergence theorem, since the phase fields are bounded between  $-1$  and  $1$  and converge pointwise.

Concerning the lim inf-inequality, for given  $\varepsilon_j \rightarrow 0$  let  $(\underline{c}_0^j, \bar{c}_0^j, \underline{c}_1^j, \bar{c}_1^j, u_0^j, u_1^j, \phi^j) \rightarrow (\underline{c}_0, \bar{c}_0, \underline{c}_1, \bar{c}_1, u_0, u_1, \phi)$  in  $\mathbb{R}^4 \times (L^1(\Omega))^2 \times w\text{-}W_{\text{id}}^{1,p}(\Omega)$ . Since  $\liminf_{j \rightarrow \infty} \mathfrak{L}_{\text{MM}}^{\varepsilon_j}[u_i^j] \geq \mathfrak{L}_{\text{MM}}^0[u_i]$ ,  $i = 0, 1$ , is a standard result and since  $\mathcal{W}$  is sequentially weakly lower semi-continuous, it remains to prove the sequential lower semi-continuity of the matching term.

We first extract a subsequence, still indexed by  $j$ , which realizes the lim inf and for which  $u_i^j \rightarrow u_i$  pointwise almost everywhere for  $i = 0, 1$ . We may assume  $|u_i^j| \leq 1$  pointwise, since this makes the lim inf even smaller. Also, it is sufficient to consider the case  $u_0, u_1 : \Omega \rightarrow \{-1, 1\}$ , since otherwise  $\liminf_{j \rightarrow \infty} \mathfrak{L}_{\text{MM}}^{\varepsilon_j}[u_i^j] = \infty$ . Finally, we may assume  $\lim_{j \rightarrow \infty} \mathfrak{I}_{\text{vol}}^{\varepsilon_j}[(\underline{c}_0^j, \bar{c}_0^j), (\underline{c}_1^j, \bar{c}_1^j), u_0^j, u_1^j, \phi^j] < \infty$  (otherwise there is nothing to prove) so that  $\mathcal{W}[\phi^j]$  is uniformly bounded for  $j$  large enough. Lemma 5.1 now implies  $u_0^j \circ \phi^j \rightarrow u_0 \circ \phi$  in  $L^1(\Omega)$  so that we have pointwise convergence for a subsequence and  $\int_{\Omega} |u_0^j \circ \phi^j - u_1^j|^2 \, dx \rightarrow \int_{\Omega} |u_0 \circ \phi - u_1|^2 \, dx$  follows by Lebesgue's convergence theorem.  $\square$

5.2 Proof of Theorem 4.3

Unlike in the previous proof, the sequential lower semi-continuity of the fitting term no longer relies on the convergence of compositions  $u_0^j \circ \phi^j$  as  $j \rightarrow \infty$ , since any deviation of the  $u_0^j$  from 1 will not be visible in the  $\Gamma$ -limit anyway. Thus, in essence we may assume  $u_0^j \circ \phi^j \rightarrow 1$ . For the other sequence of phase fields  $u_1^j$  we can derive that it must approach a perfect Ambrosio–Tortorelli profile, which then allows to estimate  $\frac{1}{\varepsilon_j} \int_{\Omega} (u_0^j \circ \phi^j - u_1^j)^2 dx$  from below (Lemma 5.2; unlike in the usual lower estimate for the Ambrosio–Tortorelli energy, we here perform a lower estimate only for a single-well type term under a constraint on the total Ambrosio–Tortorelli energy). Also the recovery sequence is more complicated this time: Not only a squeezing as in Fig. 5 (a) has to be implemented, but it also has to be ensured that potential slight deviations of  $u_0^j$  from 1 are not magnified by  $\phi^j$  (Lemma 5.5).

To simplify the notation, let an index to an energy (as in  $\mathcal{W}_{\Omega}[\phi] = \int_{\Omega} W(\mathfrak{D}\phi) dx$ ) denote the corresponding integration domain. We start with three technical lemmata before proving the  $\Gamma$ -convergence result. The following lemma will be needed to prove the lim inf-inequality. It basically states that for functions  $u : [0, \infty) \rightarrow \mathbb{R}$  with  $u(0) = 0$  and bounded Ambrosio–Tortorelli length energy  $\mathfrak{L}_{\text{AT}}^1[u]$ , the energy  $\|u - 1\|_{L^2([0, \infty))}^2$  is bounded below. Even more, as  $u$  approximates the optimal Ambrosio–Tortorelli profile (i.e.  $2\mathfrak{L}_{\text{AT}}^1[u] \approx 1$ ), the lower bound converges to 1.

**Lemma 5.2** *Let  $\Omega = [0, T]$ ,  $\delta, \xi > 0$ ,  $l \in [\delta, 1]$ , and define  $u^{\delta, \xi, T, l} \in W^{1,2}(\Omega)$  to be the unique minimizer of  $\tilde{\mathfrak{F}}[u] = \int_{\Omega} (u - l)^2 dx$  under the constraints  $u(0) \leq \delta$  and  $2\mathfrak{L}_{\text{AT}}^1[u] \leq 1 + \xi$ . Then  $\tilde{\mathfrak{F}}[u^{\delta, \xi, T, l}] \rightarrow \frac{1}{2}$  as  $\delta, \xi \rightarrow 0$ ,  $T \rightarrow \infty$ , and  $l \rightarrow 1$ .*

*Proof.* The above optimization problem is strictly convex with a closed convex domain and thus indeed admits a unique minimizer  $\hat{u} \equiv u^{\delta, \xi, T, l}$ . Its Lagrange functional is given by  $L[u, \mu, \lambda] = \tilde{\mathfrak{F}}[u] + \mu(u(0) - \delta) + \lambda(2\mathfrak{L}_{\text{AT}}^1[u] - 1 - \xi)$  with Lagrange multipliers  $\mu$  and  $\lambda$ . Since Slater’s condition is fulfilled, there are  $\hat{\mu}, \hat{\lambda} \geq 0$  such that  $\hat{u}, \hat{\mu}, \hat{\lambda}$  satisfy the corresponding Karush–Kuhn–Tucker conditions. In particular,  $\{0\} = \partial_u L[\hat{u}, \hat{\mu}, \hat{\lambda}]$ , from which we obtain the ordinary differential equation  $\hat{u}'' = \frac{\hat{\lambda}+1}{\hat{\lambda}}\hat{u} - \frac{\hat{\lambda}+l}{\hat{\lambda}}$  as well as  $\hat{u}'(T) = 0$ . Furthermore, since replacing  $\hat{u}$  by  $\max\{\delta, \hat{u}\}$  reduces  $\tilde{\mathfrak{F}}[u]$  as well as  $\mathfrak{L}_{\text{AT}}^1[u]$ , we know  $\hat{u}(0) = \delta$ . Altogether,

$$\hat{u}(x) = \frac{\hat{\lambda} + l}{\hat{\lambda} + 1} + \frac{\delta - \frac{\hat{\lambda}+l}{\hat{\lambda}+1}}{1 + \exp\left(-2\sqrt{\frac{\hat{\lambda}+1}{\hat{\lambda}}}T\right)} \exp\left(-\sqrt{\frac{\hat{\lambda} + 1}{\hat{\lambda}}}x\right) + \frac{\delta - \frac{\hat{\lambda}+l}{\hat{\lambda}+1}}{1 + \exp\left(2\sqrt{\frac{\hat{\lambda}+1}{\hat{\lambda}}}T\right)} \exp\left(\sqrt{\frac{\hat{\lambda} + 1}{\hat{\lambda}}}x\right).$$

Plugging  $\hat{u}$  back into  $\tilde{\mathfrak{F}}$  yields a value which continuously depends on  $\delta, T, l$ , and  $\hat{\lambda}$  and which satisfies  $\tilde{\mathfrak{F}}[\hat{u}] \rightarrow \frac{1}{2} \sqrt{\frac{\hat{\lambda}}{\hat{\lambda}+1}}$  for  $\delta \rightarrow 0$ ,  $T \rightarrow \infty$ , and  $l \rightarrow 1$ . Furthermore, from  $2\mathfrak{L}_{\text{AT}}^1[\hat{u}] \leq 1 + \xi$  we obtain the condition that  $\hat{\lambda} \rightarrow \infty$  as  $\delta, \xi \rightarrow 0$ ,  $T \rightarrow \infty$ , and  $l \rightarrow 1$  from which we finally deduce  $\tilde{\mathfrak{F}}[\hat{u}] \rightarrow \frac{1}{2}$ .  $\square$

The next lemma will be employed in the lim sup-inequality and gives a simple condition under which a sequence  $u^j$  of phase fields with phase field parameters  $\varepsilon_j \rightarrow 0$  indeed approximates the optimal Ambrosio–Tortorelli profile.

**Lemma 5.3** *Let  $T_j > 0$  and  $u_j : [-T_j, T_j] \rightarrow [0, 1]$  be given with  $T_j \rightarrow \infty$ ,  $u_j(0) \rightarrow 0$ ,  $u_j(T_j), u_j(-T_j) \rightarrow 1$ , and  $\mathcal{L}_{\text{AT}, [-T_j, T_j]}^1[u_j] = \frac{1}{2} \int_{-T_j}^{T_j} |u_j'|^2 + (u_j - 1)^2 \, dx \rightarrow 1$  as  $j \rightarrow \infty$ . Then there are extensions  $\tilde{u}_j$  of  $u_j$  to  $\mathbb{R}$  such that  $\tilde{u}_j - \bar{u} \rightarrow 0$  in  $W^{1,2}(\mathbb{R})$ , where  $\bar{u}(x) = 1 - \exp(-|x|)$  describes the optimal Ambrosio–Tortorelli profile.*

*Proof.* Define the extension of  $u_j$  by

$$\tilde{u}_j(x) = \begin{cases} u_j(x), & |x| \leq T_j, \\ \bar{u}(x - T_j - \log(1 - u_j(T_j))), & x > T_j, \\ \bar{u}(x - T_j + \log(1 - u_j(-T_j))), & x < -T_j \end{cases}$$

so that

$$\begin{aligned} & \lim_{j \rightarrow \infty} \frac{1}{2} \int_{\mathbb{R}} |\tilde{u}_j'|^2 + (\tilde{u}_j - 1)^2 \, dx \\ &= \lim_{j \rightarrow \infty} \frac{1}{2} \left[ \int_{-T_j}^{T_j} |u_j'|^2 + (u_j - 1)^2 \, dx + (1 - u_j(T_j)) + (1 - u_j(-T_j)) \right] = 1. \end{aligned}$$

Next, define

$$v_j = 1 - \frac{1 - \tilde{u}_j}{1 - \tilde{u}_j(0)}$$

so that  $v_j(0) = 0$  for all  $j$  and  $\frac{1}{2} \|1 - v_j\|_{W^{1,2}(\mathbb{R})}^2 = |1 - \tilde{u}_j(0)|^{-2} \frac{1}{2} \int_{\mathbb{R}} |\tilde{u}_j'|^2 + (\tilde{u}_j - 1)^2 \, dx \rightarrow 1$ .

For a subsequence we obtain  $1 - v_j \rightharpoonup 1 - v$  in  $W^{1,2}(\mathbb{R})$  for some  $v \in W_{\text{loc}}^{1,2}(\mathbb{R})$  with  $v(0) = 0$  and  $\frac{1}{2} \|1 - v\|_{W^{1,2}(\mathbb{R})}^2 \leq 1$  by the weak lower semi-continuity of the norm. However, 1 is the minimum value of the strictly convex optimization problem

$$\min_{\substack{u: \mathbb{R} \rightarrow \mathbb{R} \\ u(0)=0}} \frac{1}{2} \|1 - u\|_{W^{1,2}(\mathbb{R})}^2,$$

whose unique minimizer is  $\bar{u}$ . Hence we must have  $v = \bar{u}$  and therefore  $\frac{1}{2} \|1 - v\|_{W^{1,2}(\mathbb{R})}^2 = 1 = \lim_{j \rightarrow \infty} \frac{1}{2} \|1 - v_j\|_{W^{1,2}(\mathbb{R})}^2$ , which together with the weak convergence of  $1 - v_j$  yields  $1 - v_j \rightarrow 1 - v$  in  $W^{1,2}(\mathbb{R})$ . (This holds for the complete sequence since otherwise there would be a subsequence with  $\|v_j - \bar{u}\|_{W^{1,2}(\mathbb{R})} > \delta$  for a  $\delta > 0$  and all  $j$ . Then we could repeat the above argument to obtain the contradiction  $\|v_j - \bar{u}\|_{W^{1,2}(\mathbb{R})} \rightarrow 0$ .) Altogether,

$$\begin{aligned} \|\tilde{u}_j - \bar{u}\|_{W^{1,2}(\mathbb{R})} &\leq \|\tilde{u}_j - v_j\|_{W^{1,2}(\mathbb{R})} + \|v_j - \bar{u}\|_{W^{1,2}(\mathbb{R})} \\ &= |u_j(0)| \|1 - v_j\|_{W^{1,2}(\mathbb{R})} + \|v_j - v\|_{W^{1,2}(\mathbb{R})} \rightarrow 0 \end{aligned}$$

for  $j \rightarrow \infty$ . □

**Remark 5.4** Inspection of the above proof shows that instead of the interval  $[-T_j, T_j]$  we may just as well consider unsymmetric intervals. Then the lemma can be applied in the following way: Assume we are given a sequence  $u^j \in L^1(\Omega)$  of Ambrosio–Tortorelli phase fields with phase field parameters  $\varepsilon_j \rightarrow 0$  which approximate an edge set  $\mathcal{S}$ . That is (cf. [8, proof of Thm. 8.1]),

1.  $u^j \rightarrow 1$  in  $L^1(\Omega)$ ,
  2. for any  $x_i \in \mathcal{S}$  there is a sequence  $x_i^j \rightarrow x_i$  in  $\Omega$  with  $u^j(x_i^j) \rightarrow 0$ ,
  3.  $\mathcal{L}_{\text{AT}, O}^{\varepsilon_j}[u^j] \rightarrow \mathcal{H}^0(\mathcal{S} \cap O)$  for any compact  $O$  with  $O \cap \mathcal{S} = \text{int}(O) \cap \mathcal{S}$ .
- Then, for any compact connected  $O$  with  $O \cap \mathcal{S} = \text{int}(O) \cap \mathcal{S} = \{x_i\}$ , the function  $u_j : x \mapsto u^j(\varepsilon_j x + x_i^j)$  satisfies the conditions of Lemma 5.3 with  $\{-T_j, T_j\}$  replaced by  $\frac{1}{\varepsilon_j}(\partial O - x_i^j)$ . Letting  $\tilde{x} = \varepsilon_j x + x_i^j$  the lemma thus implies

$$\begin{aligned} & \int_O \varepsilon_j \left| (u^j)'(\tilde{x}) - \frac{1}{\varepsilon_j} \bar{u}'\left(\frac{\tilde{x} - x_i^j}{\varepsilon_j}\right) \right|^2 + \frac{1}{\varepsilon_j} \left( u^j(\tilde{x}) - \bar{u}\left(\frac{\tilde{x} - x_i^j}{\varepsilon_j}\right) \right)^2 d\tilde{x} \\ &= \int_{\frac{O - x_i^j}{\varepsilon_j}} |u_j'(x) - \bar{u}'(x)|^2 + (u_j(x) - \bar{u}(x))^2 dx \leq \|u_j - \bar{u}\|_{W^{1,2}(\mathbb{R})} \xrightarrow{j \rightarrow \infty} 0. \end{aligned}$$

Finally, the third lemma helps to ensure the existence of a recovery sequence for the deformation  $\phi$ . This recovery sequence has to be designed carefully so that the pullback  $u^j \circ \phi^j$  does not blow up spurious edges in the phase fields  $u^j$ .

**Lemma 5.5** For given  $\varepsilon_j \rightarrow 0$  and bounded  $\phi \in W^{1,p}([0, 1])$  with  $\mathcal{W}[\phi] < \infty$ , let  $v^j \in W^{1,2}([\phi(0), \phi(1)])$  with  $\frac{1}{\varepsilon_j} \int_{\phi(0)}^{\phi(1)} (v^j)^2 dx \rightarrow 0$ . Then there exists a sequence  $\phi^j \rightarrow \phi$  in  $W^{1,p}([0, 1])$  with  $\phi^j(0) = \phi(0)$  and  $\phi^j(1) = \phi(1)$  such that  $\mathcal{W}[\phi^j] \rightarrow \mathcal{W}[\phi]$  and  $\frac{1}{\varepsilon_j} \int_0^1 (v^j \circ \phi^j)^2 dx \rightarrow 0$ .

*Proof.* Due to the conditions on the hyperelastic energy density  $W$ ,  $\phi$  is absolutely continuous and thus almost everywhere differentiable, and  $\phi$  is invertible with some absolutely continuous  $\psi = \phi^{-1} : [\phi(0), \phi(1)] \rightarrow [0, 1]$ . For a positive sequence  $\delta_j \rightarrow 0$ , let  $E_j = \{x \in [\phi(0), \phi(1)] : v^j(x) > \delta_j \sqrt{\varepsilon_j}\}$  and  $A_j = \{x \in E_j : \phi'(\psi(x)) < 1\}$ . Then, if  $\delta_j$  converges slowly enough,

$$\text{vol}(E_j) = \frac{1}{\varepsilon_j} \int_{E_j} \varepsilon_j dx \leq \frac{1}{\varepsilon_j} \int_{E_j} \left(\frac{v^j}{\delta_j}\right)^2 dx \leq \frac{1}{\delta_j^2 \varepsilon_j} \int_{\phi(0)}^{\phi(1)} (v^j)^2 dx \rightarrow 0,$$

and likewise  $\text{vol}(\psi(E_j)) \rightarrow 0$ . Let  $\varphi_j = \frac{\text{vol}(\psi(A_j)) - \text{vol}(A_j)}{\text{vol}([\phi(0), \phi(1)] \setminus A_j)} \geq 0$  and define

$$\phi^j = (\psi^j)^{-1} \text{ for } \psi^j(x) = \phi(0) + \int_{\phi(0)}^x g_j(y) dy \text{ with } g_j(x) = \begin{cases} 1, & x \in A_j, \\ \psi'(x) + \varphi_j, & x \notin A_j. \end{cases}$$

The deformation  $\phi^j$  is well-defined since the absolutely continuous deformation  $\psi^j$  has positive derivative almost everywhere. Then  $\phi^j(0) = \phi(0)$ ,  $\phi^j(1) = \phi(1)$ , as well as

$$\begin{aligned} \frac{1}{\varepsilon_j} \int_0^1 (v^j \circ \phi^j)^2 dx &\leq \frac{1}{\varepsilon_j} \int_{[0,1] \setminus (\phi^j)^{-1}(E_j)} (\delta_j \sqrt{\varepsilon_j})^2 dx + \frac{1}{\varepsilon_j} \int_{(\phi^j)^{-1}(E_j)} (v^j \circ \phi^j)^2 dx \\ &\leq \delta_j^2 + \frac{1}{\varepsilon_j} \int_{E_j} (v^j)^2 dx \xrightarrow{j \rightarrow \infty} 0. \end{aligned}$$

Also,

$$\mathcal{W}[\phi^j] = \int_{\phi(0)}^{\phi(1)} W\left(\frac{1}{g_j}\right) |g_j| \, dx \xrightarrow{j \rightarrow \infty} \int_{\phi(0)}^{\phi(1)} W\left(\frac{1}{\psi'}\right) |\psi'| \, dx = \mathcal{W}[\phi],$$

where we have applied Lebesgue’s theorem since the integrand converges pointwise (due to the continuity of  $W$ ) and is bounded by a constant plus a factor times  $W(1/\psi')|\psi'|$ .<sup>2</sup> Finally, the  $\phi^j$  are uniformly bounded with  $\phi^j \rightarrow \phi$  pointwise and

$$\int_0^1 |\mathfrak{D}\phi^j|^p \, dx = \int_{\phi(0)}^{\phi(1)} \left| \frac{1}{g_j} \right|^{p-1} \, dx \leq |A_j| + \int_{[\phi(0), \phi(1)] \setminus A_j} \left| \frac{1}{\psi'} \right|^{p-1} \, dx,$$

where the second term is bounded above by  $\int_{\phi(0)}^{\phi(1)} \left| \frac{1}{\psi'} \right|^{p-1} \, dx = \int_0^1 |\mathfrak{D}\phi|^p \, dx$  so that we obtain weak convergence of a subsequence  $\phi^j \rightharpoonup \phi$  (and since we can extract such a sequence from any subsequence we obtain weak convergence of the complete sequence).  $\square$

Now we are able to prove Thm. 4.3. The underlying idea of how the phase fields and the deformation behave locally is illustrated in Fig. 5. Most work is caused by the separate treatment of the different cases in Fig. 5 to construct a recovery sequence.

*Proof of Thm. 4.3.* For the lim inf-inequality consider a sequence  $\varepsilon_j \rightarrow 0$  as well as a sequence  $\phi^j \rightharpoonup \phi$  in  $W_{\text{id}}^{1,p}(\Omega)$ . The lower semi-continuity  $\liminf_{j \rightarrow \infty} \mathcal{W}[\phi^j] \geq \mathcal{W}[\phi]$  follows from the assumptions on the hyperelastic energy density  $W$ . We may assume  $\liminf_{j \rightarrow \infty} \mathcal{W}[\phi^j] < \infty$  (otherwise the lim inf-inequality would be trivially fulfilled) so that  $\mathcal{W}[\phi] < \infty$  and  $\phi$  is a homeomorphism.

Define

$$h = \liminf_{j \rightarrow \infty} \inf_{\substack{(y_0, u_0) \in \mathfrak{m}^{\varepsilon_j}(\hat{y}_0) \\ (y_1, u_1) \in \mathfrak{m}^{\varepsilon_j}(\hat{y}_1)}} \frac{1}{\varepsilon_j} \int_{\Omega} (u_0 \circ \phi^j - u_1)^2 \, dx.$$

Upon taking a subsequence (and after reindexing), we may assume that the lim inf can be replaced by a lim. Let  $(y_i^j, u_i^j) \in \mathfrak{m}^{\varepsilon_j}(\hat{y}_i)$ ,  $i = 0, 1$ , be sequences of images and phase fields such that the inner infimum in the definition of  $h$  is realized up to  $2^{-j}$  so that finally

$$h = \lim_{j \rightarrow \infty} \frac{1}{\varepsilon_j} \int_{\Omega} (u_0^j \circ \phi^j - u_1^j)^2 \, dx.$$

By the  $\Gamma$ -convergence and equi-mild coercivity of  $\mathcal{E}_{\text{AT}}^{\hat{y}_i, \varepsilon_j}$  (cf. [8, Def. 1.19 to Thm. 1.21]), we may (again after extracting a subsequence without reindexing) assume  $(y_i^j, u_i^j) \rightarrow (y_i, 1)$  in  $(L^1(\Omega))^2$  and pointwise a. e. for  $i = 0, 1$ , where  $y_i$  is a solution of the respective Mumford–Shah problem. Even more, inspecting the proof for  $\Gamma$ -convergence of  $\mathcal{E}_{\text{AT}}^{\hat{y}_i, \varepsilon_j}$  (e.g. [8, Thm. 8.1]), we have  $\mathcal{L}_{\text{AT}}^{\varepsilon_j}[u_i^j] \rightarrow \mathcal{H}^0(\mathcal{S}_{y_i})$  as  $j \rightarrow \infty$ , and for every  $x_m \in \mathcal{S}_{y_1} \setminus \phi^{-1}(\mathcal{S}_{y_0})$  there exist a sequence  $x_m^j \rightarrow x_m$  and  $T < \frac{\hat{T}}{2}$ , where  $\hat{T}$  is the minimum distance between any two elements of

<sup>2</sup> Note that  $\varphi_j \leq 1$  and that  $s \mapsto W(\frac{1}{s})s$  is non-negative and convex on  $(0, \infty)$  with minimum at  $s = 1$ . Thus, for  $\psi' < 1$  we have  $W(\frac{1}{\psi'+\varphi_j})|\psi'+\varphi_j| \leq \max(W(\frac{1}{\psi'})|\psi'|, W(\frac{1}{2})2)$ , and for  $\psi' \geq 1$  we may assume  $W(\frac{1}{\psi'+\varphi_j})|\psi'+\varphi_j|$  less than some constant times  $W(1/\psi')|\psi'|$  due to the growth conditions on  $W$ .

$\mathcal{S}_{y_1} \cup \phi^{-1}(\mathcal{S}_{y_0})$ , such that  $u_1^j(x_m^j) \rightarrow 0$  and  $\text{ess inf}_{x \in \phi^j([x_m^j - T, x_m^j + T])} u_0^j(x) \rightarrow 1$  (where we have exploited the convergence  $\phi^j \rightarrow \phi$  in  $C^0(\overline{\Omega})$ ).

We now introduce the rescaled functions

$$\begin{aligned} \tilde{u}_1^j(x) &= u_1^j(x_m^j + \varepsilon_j x), \\ \tilde{u}_0^j(x) &= u_0^j(\phi^j(x_m^j) + \varepsilon_j x), \\ \tilde{\phi}^j(x) &= \frac{1}{\varepsilon_j} [\phi^j(x_m^j + \varepsilon_j x) - \phi^j(x_m^j)] \end{aligned}$$

so that  $\liminf_{j \rightarrow \infty} \frac{1}{\varepsilon_j} \int_{x_m^j - T}^{x_m^j + T} (u_0^j \circ \phi^j - u_1^j)^2 dx = \liminf_{j \rightarrow \infty} \int_{-\frac{T}{\varepsilon_j}}^{\frac{T}{\varepsilon_j}} (\tilde{u}_0^j \circ \tilde{\phi}^j - \tilde{u}_1^j)^2 dx \geq 1$ , where the inequality follows by Lemma 5.2. Hence,

$$h \geq \liminf_{j \rightarrow \infty} \sum_{x_m \in \mathcal{S}_{y_1} \setminus \phi^{-1}(\mathcal{S}_{y_0})} \frac{1}{\varepsilon_j} \int_{x_m^j - T}^{x_m^j + T} (u_0^j \circ \phi^j - u_1^j)^2 dx \geq \mathcal{H}^0(\mathcal{S}_{y_1} \setminus \phi^{-1}(\mathcal{S}_{y_0})),$$

which concludes the lim inf-inequality.

For the recovery sequence, assume  $\phi \in W_{\text{id}}^{1,p}(\Omega)$  and  $\varepsilon_j \rightarrow 0$  to be given. Choose  $y_i \in \mathfrak{m}^0(\hat{y}_i)$ ,  $i = 0, 1$ , such that the infimum in  $\mathcal{G}^0[\phi]$  is realized up to  $\delta > 0$ . Then there are corresponding  $(y_i^j, u_i^j) \in \mathfrak{m}^{\varepsilon_j}(\hat{y}_i)$  with  $(y_i^j, u_i^j) \rightarrow (y_i, 1)$  in  $(L^1(\Omega))^2$ ,  $i = 0, 1$ .

Since the  $(y_i^j, u_i^j)$  are a converging sequence of minimizers of the  $\Gamma$ -converging sequence of Ambrosio–Tortorelli functionals, we have  $\mathcal{L}_{\text{AT}}^{\varepsilon_j}[u_i^j] \rightarrow \mathcal{H}^0(\mathcal{S}_{y_i})$ , and for each  $x_i \in \mathcal{S}_{y_i}$ ,  $i = 0, 1$ , we know there is a sequence  $x_i^j \rightarrow x_i$  with  $u_i^j(x_i^j) \rightarrow 0$ . Remark 5.4 then implies that the  $u_i^j$  approximate the optimal Ambrosio–Tortorelli profile on any compact  $O \subset \Omega$  containing only one element of  $\mathcal{S}_{y_i}$ .

Let  $T$  be half the minimum distance between any two points in  $\mathcal{S}_{y_1} \cup \phi^{-1}(\mathcal{S}_{y_0})$ . We divide the domain  $\Omega$  into four different types of regions: Intervals  $[x_1 - T, x_1 + T] \cap \Omega$  with  $x_1 \in \mathcal{S}_{y_1} \setminus \phi^{-1}(\mathcal{S}_{y_0})$ , intervals  $[x_0 - T, x_0 + T] \cap \Omega$  with  $x_0 \in \phi^{-1}(\mathcal{S}_{y_0}) \setminus \mathcal{S}_{y_1}$ , intervals  $[x - T, x + T] \cap \Omega$  with  $x \in \phi^{-1}(\mathcal{S}_{y_0}) \cap \mathcal{S}_{y_1}$ , and the remainder  $\tilde{\Omega}$ , which itself is composed of a finite number of intervals. For each type of interval we locally define a deformation  $\phi^j$  and show convergence  $\phi^j \rightarrow \phi$  and convergence of the deformation energy and the mismatch term separately:

- For each interval  $[x_l, x_r] \subset \tilde{\Omega}$  Remark 5.4 implies

$$\frac{1}{\varepsilon_j} \int_{x_l}^{x_r} (u_1^j - 1)^2 dx \rightarrow 0 \quad \text{and} \quad \frac{1}{\varepsilon_j} \int_{\phi(x_l)}^{\phi(x_r)} (u_0^j - 1)^2 dx \rightarrow 0.$$

Lemma 5.5 then implies the existence of a sequence  $\phi^j : [x_l, x_r] \rightarrow [\phi(x_l), \phi(x_r)]$  with  $\phi^j \rightarrow \phi$  and  $\mathcal{W}_{[x_l, x_r]}[\phi^j] \rightarrow \mathcal{W}_{[x_l, x_r]}[\phi]$  such that for  $j \rightarrow \infty$ ,

$$\sqrt{\frac{1}{\varepsilon_j} \int_{x_l}^{x_r} (u_0^j \circ \phi^j - u_1^j)^2 dx} \leq \sqrt{\frac{1}{\varepsilon_j} \int_{x_l}^{x_r} (u_0^j \circ \phi^j - 1)^2 dx} + \sqrt{\frac{1}{\varepsilon_j} \int_{x_l}^{x_r} (1 - u_1^j)^2 dx} \rightarrow 0.$$

- On any  $[x_1 - T, x_1 + T]$  with  $x_1 \in \mathcal{S}_{y_1} \setminus \phi^{-1}(\mathcal{S}_{y_0})$  we analogously define  $\phi^j \rightarrow \phi$  in  $W^{1,p}([x_1 -$

$T, x_1 + T)$  with  $\mathcal{W}_{[x_1-T, x_1+T]}[\phi^j] \rightarrow \mathcal{W}_{[x_1-T, x_1+T]}[\phi]$  such that

$$\begin{aligned} \sqrt{\frac{1}{\varepsilon_j} \int_{x_1-T}^{x_1+T} (u_0^j \circ \phi^j - u_1^j)^2 dx} &\leq \sqrt{\frac{1}{\varepsilon_j} \int_{x_1-T}^{x_1+T} (u_0^j \circ \phi^j - 1)^2 dx} \\ &\quad + \sqrt{\frac{1}{\varepsilon_j} \int_{x_1-T}^{x_1+T} (1 - u_1^j)^2 dx} \rightarrow 0 + 1 \end{aligned}$$

for  $j \rightarrow \infty$ , where the convergence of the second term again follows from the convergence of  $u_1^j$  against the optimal profile around  $x_1$  (Remark 5.4).

- For each interval  $O = [x_0 - T, x_0 + T]$  with  $x_0 \in \phi^{-1}(\mathcal{S}_{y_0}) \setminus \mathcal{S}_{y_1}$  we define  $\phi^j(x) = \phi(x_0) + \varepsilon_j^{-\beta}(x - x_0)$  for  $|x - x_0| < \varepsilon_j^\alpha$ , where  $1 > \alpha > \beta, r\beta > 0$  (here, again,  $r$  is the exponent from the growth conditions on  $W$ ). A slight modification of Lemma 5.5 then implies that  $\phi^j$  can be extended onto  $O_j = [x_0 - T, x_0 + T] \setminus [x_0 - \varepsilon_j^\alpha, x_0 + \varepsilon_j^\alpha]$  so that still  $\phi^j \rightarrow \phi$  and  $\mathcal{W}_{O_j}[\phi^j] \rightarrow \mathcal{W}_O[\phi]$  (while  $\mathcal{W}_{[x_0-\varepsilon_j^\alpha, x_0+\varepsilon_j^\alpha]}[\phi^j] \leq 2\varepsilon_j^\alpha(C_1 + C_2\varepsilon_j^{-r\beta}) \rightarrow 0$ ) as well as

$$\begin{aligned} &\sqrt{\frac{1}{\varepsilon_j} \int_O (u_0^j \circ \phi^j - u_1^j)^2 dx} \\ &\leq \sqrt{\frac{1}{\varepsilon_j} \int_O (u_0^j \circ \phi^j - 1)^2 dx} + \sqrt{\frac{1}{\varepsilon_j} \int_O (1 - u_1^j)^2 dx} \\ &= \sqrt{\varepsilon_j^\beta \frac{1}{\varepsilon_j} \int_{\phi(x_0)-\varepsilon_j^{\alpha-\beta}}^{\phi(x_0)+\varepsilon_j^{\alpha-\beta}} (u_0^j - 1)^2 dx} + \frac{1}{\varepsilon_j} \int_{O_j} (u_0^j \circ \phi^j - 1)^2 dx \\ &\quad + \sqrt{\frac{1}{\varepsilon_j} \int_O (1 - u_1^j)^2 dx} \rightarrow 0. \end{aligned}$$

- Finally, for each interval  $O = [x_1 - T, x_1 + T]$  with  $x_1 \in \phi^{-1}(\mathcal{S}_{y_0}) \cap \mathcal{S}_{y_1}$  let  $x_0^j \rightarrow \phi(x_1)$  and  $x_1^j \rightarrow x_1$  be sequences such that  $u_0^j(x_0^j) \rightarrow 0$  and  $u_1^j(x_1^j) \rightarrow 0$ . We define  $\phi^j(x) = \phi(x_1^j) + x - x_0^j$  for  $|x - x_0^j| < \varepsilon_j^\alpha$ , where  $1 > \alpha > 0$ . As in the previous case we can extend  $\phi^j$  onto  $O_j = [x_0 - T, x_0 + T] \setminus [x_0^j - \varepsilon_j^\alpha, x_0^j + \varepsilon_j^\alpha]$  so that  $\phi^j \rightarrow \phi$  and  $\mathcal{W}_{O_j}[\phi^j] \rightarrow \mathcal{W}_O[\phi]$  and

$$\frac{1}{\varepsilon_j} \int_O (u_0^j \circ \phi^j - u_1^j)^2 dx = \frac{1}{\varepsilon_j} \int_{x_0^j - \varepsilon_j^\alpha}^{x_0^j + \varepsilon_j^\alpha} (u_0^j \circ \phi^j - u_1^j)^2 dx + \frac{1}{\varepsilon_j} \int_{O_j} (u_0^j \circ \phi^j - u_1^j)^2 dx,$$

where the first term converges to zero since  $u_0^j(\phi(x_1^j) + x - x_0^j)$  and  $u_1^j(x)$  approach the same profile (Remark 5.4), and the second term can be shown to converge to zero as done before on the intervals in  $\tilde{\Omega}$ .

Altogether we obtain

$$\begin{aligned} \limsup_{j \rightarrow \infty} \mathfrak{g}^{\varepsilon_j}[\phi^j] &\leq \limsup_{j \rightarrow \infty} \mathcal{W}[\phi^j] + \frac{1}{\varepsilon_j} \int_{\Omega} (u_0^j \circ \phi^j - u_1^j)^2 dx = \mathcal{W}[\phi] + \mathcal{H}^{d-1}(\mathcal{S}_{y_1} \setminus \phi^{-1}(\mathcal{S}_{y_0})) \\ &\leq \mathfrak{g}^0[\phi] + \delta, \end{aligned}$$

which by the arbitrariness of  $\delta$  concludes the proof. □

5.3 Proof of Theorem 4.5

The lim inf inequality is more or less standard except for the mismatch term  $\mathcal{F}$  and the Ambrosio–Tortorelli length terms  $\mathcal{L}_{AT}^\varepsilon$  in the vicinity of  $\phi(\mathcal{S}_{y_1}) \setminus \mathcal{S}_{y_0}$  as in Fig. 6(c). Here, the mismatch term has to be viewed as a modification of the potential in  $\mathcal{L}_{AT}^\varepsilon$ , which results in a different lower bound than for  $\mathcal{L}_{AT}^\varepsilon$  alone. This lower bound can be obtained quite explicitly by globally minimizing the modified Ambrosio–Tortorelli length terms for the optimal profile (Lemmas 5.6 and 5.7).

As opposed to the previous section, the recovery sequence this time also has to provide the phase fields. Again, while the phase field sequences  $u_0^j, u_1^j$  are the standard Ambrosio–Tortorelli recovery sequences for the cases in Fig. 6(a),(b), both  $u_0^j$  and  $u_1^j$  are non-standard for the situation in Fig. 6(c). In that latter case they can be explicitly characterized as the above-mentioned optimal profiles. The recovery sequence for the deformations is essentially the same as in the previous section, only it can now easily be made very explicit since this time we are given the exact profiles of the phase fields to be matched. Therefore we do not need to refer to Lemma 5.5 here.

First, we consider the function  $Z^{0,1}$ . Its well-definedness and its properties follow from the next two lemmata.

**Lemma 5.6** *Let  $1 \geq l \geq \kappa \geq 0$  and define*

$$Y^{\kappa,l} = \{u \in W^{1,2}((0, \infty)) : u(0) = \kappa, l \leq \operatorname{ess\,sup}_{x \geq 0} u(x)\}.$$

*For  $u \in Y^{\kappa,l}$  we introduce the abbreviation  $x_u^l = \min\{x \geq 0 : u(x) = l\}$  if  $l \in u((0, \infty))$  and  $x_u^l = \infty$  else (note that point values of  $u$  are well-defined due to the embedding  $W^{1,2}((0, \infty)) \hookrightarrow C^0([0, \infty))$ ). Then for  $a \geq 0$  the variational problem*

$$\min_{u \in Y^{\kappa,l}} U^{\kappa,l,a}[u], \quad U^{\kappa,l,a}[u] = \int_0^{x_u^l} |u'|^2 + (1-u)^2 + 2a(l-u)^2 \, dx,$$

*admits minimizers. All minimizers  $u$  have the same  $x_u^l$  and coincide on  $[0, x_u^l]$  with a strictly increasing, concave, and smooth function  $\bar{u}$ . Finally,  $U^{\kappa,l,a}[\bar{u}] = \bar{U}^{\kappa,l,a}$  for  $\bar{U}^{\kappa,l,a} = 2 \int_\kappa^l \sqrt{(1-z)^2 + 2a(l-z)^2} \, dz$ .*

*Proof.* To compute a lower bound on  $U^{\kappa,l,a}$ , consider an arbitrary function  $u \in Y^{\kappa,l}$ . We may assume  $u$  to be strictly increasing on  $(0, x_u^l)$  since otherwise there would be  $0 < x_1 < x_2 < x_u^l$  with  $u(x_1) = u(x_2)$  so that we could replace  $u$  on  $[x_1, \infty)$  by  $x \mapsto u(x-x_1+x_2)$ , thereby reducing  $U^{\kappa,l,a}$ . By the continuity and monotonicity of  $u : (0, x_u^l) \rightarrow (\kappa, l)$ ,  $u$  is invertible so that the change of variables  $z = u(x)$  yields

$$U^{\kappa,l,a}[u] = \int_\kappa^l u' \circ u^{-1}(z) + \frac{(1-z)^2 + 2a(l-z)^2}{u' \circ u^{-1}(z)} \, dz \geq 2 \int_\kappa^l \sqrt{(1-z)^2 + 2a(l-z)^2} \, dz = \bar{U}^{\kappa,l,a},$$

where equality holds if and only if  $u' \circ u^{-1}(z) = \sqrt{(1-z)^2 + 2a(l-z)^2}$  almost everywhere on  $(\kappa, l)$ , which is equivalent to  $u' = \sqrt{(1-u)^2 + 2a(l-u)^2}$ . Since the right hand side of this ordinary differential equation is Lipschitz continuous, there is a unique solution  $\bar{u}$  to it. This  $\bar{u}$  is obviously strictly increasing and concave.  $\square$

By a change of variables we obtain  $x_u^l = \int_0^{x_u^l} dx = \int_\kappa^l \sqrt{(1-u)^2 + 2a(l-u)^2}^{-1} du$ , which smoothly depends on  $\kappa, l$ , and  $a$ . Likewise,  $\bar{U}^{\kappa,l,a}$  depends smoothly on  $\kappa, l$ , and  $a$  with  $\bar{U}^{\kappa,l,0} = 2(l-\kappa) - (l^2 - \kappa^2)$  and  $\bar{U}^{\kappa,l,a} \sim \sqrt{2a}(l-\kappa)^2$  as  $a \rightarrow \infty$ .

**Lemma 5.7** *Given  $0 \leq \kappa \leq \lambda \leq 1$ , the variational problem*

$$\min_{l \in [\kappa, \lambda]} V^{\kappa, \lambda, a}[l], \quad V^{\kappa, \lambda, a}[l] = \bar{U}^{\kappa, l, a} + 4 \int_l^\lambda 1 - z \, dz - 1$$

has a unique solution  $\bar{l} \in [\kappa, \lambda]$ , which depends continuously on  $\kappa$ ,  $\lambda$ , and  $a$ . The minimum value  $Z^{\kappa, \lambda}(a)$  is also continuous in  $\kappa$ ,  $\lambda$ , and  $a$ .

*Proof.* The derivative of  $\bar{U}^{\kappa, l, a}$  with respect to  $l$  is given by

$$\partial_l \bar{U}^{\kappa, l, a} = 2 - 2l + 2 \int_\kappa^l \frac{2a(l - z)}{\sqrt{(1 - z)^2 + 2a(l - z)^2}} \, dz,$$

where the integrand is increasing in  $l$  and thus the second derivative must be greater than  $-2$ . Since the second derivative of  $4 \int_l^\lambda 1 - z \, dz$  is 4, the functional  $V^{\kappa, \lambda, a}$  is strictly convex so that a unique minimum  $\bar{l}$  is attained on the compact interval  $[\kappa, \lambda]$ .

To show that  $\bar{l}$  depends continuously on  $\kappa$ ,  $\lambda$ , and  $a$ , note that the first derivative of  $V^{\kappa, \lambda, a}[l]$  with respect to  $l$  is smooth in  $\kappa$ ,  $\lambda$ , and  $a$ . If this derivative is zero at  $\bar{l}$ , then by the implicit function theorem,  $\bar{l}$  is locally a smooth function of  $\kappa$ ,  $\lambda$ , and  $a$ . Else, if  $\bar{l} = \kappa$  (meaning  $\partial_l V^{\kappa, \lambda, a}[l] > 0$  on  $[\kappa, \lambda]$ ), then a small perturbation of  $\kappa$ ,  $\lambda$ , or  $a$  will preserve the positivity of  $\partial_l V^{\kappa, \lambda, a}[l]$  and thus  $\bar{l} = \kappa$ . Continuity of  $\bar{l}$  at  $\bar{l} = \lambda$  is shown analogously.

The continuity of  $Z^{\kappa, \lambda}(a)$  follows from the continuity of  $V^{\kappa, \lambda, a}[l]$  in  $\kappa$ ,  $\lambda$ ,  $a$ , and  $l$  combined with the continuity of  $\bar{l}$  in  $\kappa$ ,  $\lambda$ , and  $a$ . □

For  $a = 0$ , it is easy to validate  $\bar{l} = \lambda$  and  $Z^{\kappa, \lambda}(0) = 2(\lambda - \kappa) - (\lambda^2 - \kappa^2) - 1$ , while for  $a \rightarrow \infty$  a simple calculation shows  $\bar{l} = \kappa$  with  $Z^{\kappa, \lambda}(\infty) = 4(\lambda - \kappa) - 2(\lambda^2 - \kappa^2) - 1$ . To obtain the derivative  $(Z^{0,1})'(0)$ , note

$$\begin{aligned} (Z^{0,1})'(a) &= \partial_a V^{0,1,a}[\bar{l}] + \partial_l V^{0,1,a}[\bar{l}] \partial_a \bar{l} \\ &= 2 \int_0^{\bar{l}} \frac{(\bar{l} - z)^2}{\sqrt{(1 - z)^2 + 2a(\bar{l} - z)^2}} \, dz + \left( 2\bar{l} - 2 + 2 \int_0^{\bar{l}} \frac{2a(\bar{l} - z)}{\sqrt{(1 - z)^2 + 2a(\bar{l} - z)^2}} \, dz \right) \partial_a \bar{l}, \end{aligned}$$

which for  $a = 0$  and thus  $\bar{l} = 1$  becomes 1. The function is displayed in Fig. 7. We now successively prove the lim inf- and the lim sup-inequality from Thm. 4.5.

*Proof of Thm. 4.5, lim inf-inequality.* The fidelity terms  $\int_\Omega (y_i - \hat{y}_i)^2 \, dx$  just represent continuous perturbations of the functional and can thus be neglected.

Let  $\varepsilon_j \rightarrow 0$  be given and consider a sequence  $(y_0^j, y_1^j, u_0^j, u_1^j, \phi^j)$  which converges against  $(y_0, y_1, u_0, u_1, \phi)$  in  $(L^1(\Omega))^4 \times w - W_{\text{id}}^{1,p}(\Omega)$ . As usual, we may extract a subsequence, still indexed by  $j$ , so that this convergence is also pointwise a. e. and the energy converges against the lim inf, where this limit may be assumed finite (there is nothing to prove otherwise). Furthermore, as before we may assume  $0 \leq u_0^j, u_1^j \leq 1$  pointwise, since this reduces the lim inf even further. By the conditions on  $\mathcal{W}$  we have  $\liminf_{j \rightarrow \infty} \mathcal{W}[\phi^j] \geq \mathcal{W}[\phi]$ , and  $\liminf_{j \rightarrow \infty} \int_\Omega (u_i^j)^2 |\nabla y_i^j|^2 \, dx \geq \int_{\Omega \setminus \mathcal{S}_{y_i}} |\nabla y_i|^2 \, dx$  follows by the standard argument for the Ambrosio–Tortorelli segmentation. Furthermore, by the properties of  $\mathcal{W}$ ,  $\phi$  is a homeomorphism. It remains to examine the behavior of the length regularization and the matching term.

Due to the finiteness of  $\mathcal{S}_{y_0}$  and  $\mathcal{S}_{y_1}$  there exists  $\eta > 0$  such that the open  $\eta$ -neighborhood  $V_\eta = B_\eta(\mathcal{S}_{y_1} \setminus \phi^{-1}(\mathcal{S}_{y_0}))$  satisfies  $\phi(V_\eta) \cap B_\eta(\mathcal{S}_{y_0}) = \emptyset$  (note that  $\phi^{-1}(\mathcal{S}_{y_0})$  is compact due to the continuity of  $\phi$ ). Again letting an index to an energy functional denote the integration domain, by the standard Ambrosio–Tortorelli argument we have

$$\begin{aligned} \liminf_{j \rightarrow \infty} \frac{a}{\varepsilon_j} \mathfrak{F}_{\Omega \setminus V_\eta}[u_0^j, u_1^j, \phi^j] + \nu \mathfrak{L}_{\text{AT}, \Omega \setminus \phi(V_\eta)}^{\varepsilon_j}[u_0^j] + \nu \mathfrak{L}_{\text{AT}, \Omega \setminus V_\eta}^{\varepsilon_j}[u_1^j] \\ \geq 0 + \nu \mathcal{H}^0(\mathcal{S}_{y_0} \cap (\Omega \setminus \phi(V_\eta))) + \nu \mathcal{H}^0(\mathcal{S}_{y_1} \cap (\Omega \setminus V_\eta)), \end{aligned}$$

so it suffices to consider the remainder,

$$E^j[u_0^j, u_1^j, \phi^j] = \frac{a}{\varepsilon_j} \mathfrak{F}_{V_\eta}[u_0^j, u_1^j, \phi^j] + \nu \mathfrak{L}_{\text{AT}, \phi(V_\eta)}^{\varepsilon_j}[u_0^j] + \nu \mathfrak{L}_{\text{AT}, V_\eta}^{\varepsilon_j}[u_1^j].$$

For simplicity, let us assume that  $V_\eta \cap \mathcal{S}_{y_1}$  only contains one single element  $x_c$  (otherwise split  $V_\eta$  into several intervals and apply the following argument to all of them). As in the standard proof for the  $\Gamma$ -convergence of the Ambrosio–Tortorelli energy [8, Thm. 8.1], we know there are sequences  $x_l^j < x_c^j < x_r^j$  in  $V_\eta$  with  $x_l^j, x_c^j, x_r^j \rightarrow x_c$  and  $u_1^j(x_l^j), u_1^j(x_r^j) \rightarrow 1, u_1^j(x_c^j) \rightarrow 0$ . Likewise we know  $u_0^j \rightarrow 1$  almost everywhere so that there are  $x_l, x_r \in \phi(V_\eta)$  with  $x_l < \phi(x_c) < x_r$  and  $u_0^j(x_l), u_0^j(x_r) \rightarrow 1$ . Denote the essential infimum of  $u_0^j$  on  $(x_l, x_r)$  by  $l^j \in [0, 1]$ . Obviously,

$$\begin{aligned} E^j[u_0^j, u_1^j, \phi^j] &\geq \frac{a}{\varepsilon_j} \int_{V_\eta \cap \{u_1^j \leq l^j\}} |l^j - u_1^j|^2 dx + \nu \mathfrak{L}_{\text{AT}, [x_l, x_r]}^{\varepsilon_j}[u_0^j] + \nu \mathfrak{L}_{\text{AT}, V_\eta \cap \{u_1^j \leq l^j\}}^{\varepsilon_j}[u_1^j] \\ &\quad + \nu \mathfrak{L}_{\text{AT}, V_\eta \cap \{u_1^j > l^j\}}^{\varepsilon_j}[u_1^j] \\ &= R^j[u_0^j, u_1^j, \phi^j]. \end{aligned}$$

We may assume  $u_1^j(x_c^j)$  to be the minimum of  $u_1^j$  on  $V_\eta$  and that  $l^j \geq u_1^j(x_c^j)$  since otherwise we could replace  $u_0^j$  by  $\max\{u_0^j, u_1^j(x_c^j)\}$  so that  $R^j[u_0^j, u_1^j, \phi^j]$  becomes even smaller. For a similar reason we may assume  $u_1^j$  to be monotonic left and right of  $x_c^j$ , and  $l^j \leq u_1^j(x_l^j), u_1^j(x_r^j)$ . Using the well-known fact  $\frac{1}{2} \int_{[\underline{x}, \bar{x}]} \varepsilon |\nabla u|^2 + \frac{1}{\varepsilon} (1 - u)^2 dx \geq \left| \int_{u(\underline{x})}^{u(\bar{x})} 1 - z dz \right|$ , the second and last term in  $R^j[u_0^j, u_1^j, \phi^j]$  are bounded below by

$$2\nu \int_{l^j}^{\min\{u_0^j(x_l), u_0^j(x_r)\}} 1 - z dz + 2\nu \int_{l^j}^{\min\{u_1^j(x_l^j), u_1^j(x_r^j)\}} 1 - z dz.$$

Furthermore, upon rescaling  $z = \frac{x}{\varepsilon_j}$  and setting  $v_i(z) = u_i^j(\varepsilon_j z - x_c^j)$ ,  $[\underline{x}, \bar{x}] = \left(\frac{1}{\varepsilon_j} V_\eta - \frac{x_c^j}{\varepsilon_j}\right) \cap \{v_1 \leq l^j\}$ , the first and third term in  $R^j[u_0^j, u_1^j, \phi^j]$  become

$$\begin{aligned} \frac{\nu}{2} \int_{\underline{x}}^{\bar{x}} 2 \frac{a}{\nu} |l^j - v_1|^2 + |\nabla v_1|^2 + (1 - v_1)^2 dz &= \frac{\nu}{2} \int_{\underline{x}}^{\bar{x}} 2 \frac{a}{\nu} |l^j - v_1|^2 + |\nabla v_1|^2 + (1 - v_1)^2 dz \\ + \frac{\nu}{2} \int_0^{\bar{x}} 2 \frac{a}{\nu} |l^j - v_1|^2 + |\nabla v_1|^2 + (1 - v_1)^2 dz &\geq 2\nu \int_{u_1^j(x_c^j)}^{l^j} \sqrt{(1 - z)^2 + 2 \frac{a}{\nu} (l^j - z)^2} dz, \end{aligned}$$

where the inequality follows from Lemma 5.6. Altogether, abbreviating  $\lambda^j = \min\{u_1^j(x_l^j), u_1^j(x_r^j), u_0^j(x_l), u_0^j(x_r)\}$  and  $\kappa^j = u_1^j(x_c^j)$  we obtain

$$E^j[u_0^j, u_1^j, \phi^j] \geq 2\nu \int_{\kappa^j}^{l^j} \sqrt{(1-z)^2 + 2\frac{a}{\nu}(l^j-z)^2} dz + 4\nu \int_{l^j}^{\lambda^j} 1-z dz \geq \nu Z^{\kappa^j, \lambda^j}(\frac{a}{\nu}) + \nu,$$

where  $Z^{\kappa^j, \lambda^j}$  is defined in Lemma 5.7. By  $Z^{\kappa^j, \lambda^j}(\frac{a}{\nu}) \rightarrow Z^{0,1}(\frac{a}{\nu})$  for  $j \rightarrow \infty$ , we obtain

$$\begin{aligned} \liminf_{j \rightarrow \infty} E^j[u_0^j, u_1^j, \phi^j] &\geq \nu Z^{0,1}(\frac{a}{\nu}) + \nu \\ &= \nu Z^{0,1}(\frac{a}{\nu}) \mathcal{H}^0(\phi(\mathcal{S}_{y_1}) \setminus \mathcal{S}_{y_0}) + \nu \mathcal{H}^0(\mathcal{S}_{y_0} \cap \phi(V_\eta)) + \nu \mathcal{H}^0(\mathcal{S}_{y_1} \cap V_\eta), \end{aligned}$$

which concludes the proof. □

*Proof of Thm. 4.5, lim sup-inequality.* As before, the fidelity terms can be neglected. Let  $\varepsilon_j \rightarrow 0$  and  $(y_0, y_1, u_0, u_1, \phi) \in (L^1(\Omega))^4 \times w - W^{1,p}(\Omega)$  be given with finite energy  $\mathfrak{J}_{\text{edge}}^0$ , i.e. we can assume  $u_0, u_1 = 1$  almost everywhere,  $y_0, y_1 \in \text{pw} - W^{1,2}(\Omega)$  with  $\mathcal{S}_{y_0}, \mathcal{S}_{y_1}$  finite and  $\phi : \Omega \rightarrow \Omega$  a homeomorphism. Hence there is  $\eta > 0$  such that for each  $x \in \mathcal{S}_{y_1} \cup \phi^{-1}(\mathcal{S}_{y_0})$  we have  $V_x = [x - \eta, x + \eta] \subset \Omega$  and  $V_x \cap (\mathcal{S}_{y_1} \cup \phi^{-1}(\mathcal{S}_{y_0})) = \{x\}$ . Without loss of generality assume  $V = \bigcup_{x \in \mathcal{S}_{y_1} \cup \phi^{-1}(\mathcal{S}_{y_0})} V_x = V_0 = [-\eta, \eta]$  and  $\phi^{-1}(0) = 0$  (else apply an analogous construction as the following on each single connected component  $V_x$  of  $V$ ). Again, the same four cases as in the previous section have to be considered.

- Outside  $V$  we define the recovery sequence for  $(y_1, u_1, \phi)$  to be given by the constant sequence. Likewise, outside the  $\phi(V)$ , we take the constant sequence for  $(y_0, u_0)$ . Then abbreviating  $\mathfrak{E}_{\text{AT}}^\varepsilon[y, u] = \int_\Omega (u^2 + k_\varepsilon) |\nabla y|^2 + \nu \mathfrak{L}_{\text{AT}}^\varepsilon[u]$  we trivially have

$$\begin{aligned} \limsup_{j \rightarrow \infty} \mathfrak{E}_{\text{AT}, \Omega \setminus \phi(V)}^{\varepsilon_j}[y_0^j, u_0^j] + \mathfrak{E}_{\text{AT}, \Omega \setminus V}^{\varepsilon_j}[y_1^j, u_1^j] + \frac{a}{\varepsilon_j} \mathfrak{F}_{\Omega \setminus V}[u_0^j, u_1^j, \phi^j] + \mathcal{W}_{\Omega \setminus V}[\phi^j] \\ \leq \int_{\Omega \setminus \phi(V)} |\nabla y_0|^2 dx + \int_{\Omega \setminus V} |\nabla y_1|^2 dx + \mathcal{W}_{\Omega \setminus V}[\phi]. \end{aligned}$$

It remains to find a recovery sequence  $(y_1^j, u_1^j, \phi^j)$  on  $V_x$  and  $(y_0^j, u_0^j)$  on  $\phi(V_x)$  for each  $x \in \mathcal{S}_{y_1} \cup \phi^{-1}(\mathcal{S}_{y_0})$ , which is consistent with the function values on  $\Omega \setminus V$  and  $\Omega \setminus \phi(V)$ , respectively, and which satisfies

$$\begin{aligned} \limsup_{j \rightarrow \infty} \mathfrak{E}_{\text{AT}, \phi(V_x)}^{\varepsilon_j}[y_0^j, u_0^j] + \mathfrak{E}_{\text{AT}, V_x}^{\varepsilon_j}[y_1^j, u_1^j] + \frac{a}{\varepsilon_j} \mathfrak{F}_{V_x}[u_0^j, u_1^j, \phi^j] + \mathcal{W}_{V_x}[\phi^j] \\ \leq \mathcal{W}_{V_x}[\phi] + \begin{cases} \int_{\phi(V_x \setminus \{x\})} |\nabla y_0|^2 dx + \int_{V_x \setminus \{x\}} |\nabla y_1|^2 dx + 2\nu, & \text{if } x \in \phi^{-1}(\mathcal{S}_{y_0}) \cap \mathcal{S}_{y_1}, \\ \int_{\phi(V_x \setminus \{x\})} |\nabla y_0|^2 dx + \int_{V_x} |\nabla y_1|^2 dx + \nu, & \text{if } x \in \phi^{-1}(\mathcal{S}_{y_0}) \setminus \mathcal{S}_{y_1}, \\ \int_{\phi(V_x)} |\nabla y_0|^2 dx + \int_{V_x \setminus \{x\}} |\nabla y_1|^2 dx + \nu + \nu Z^{0,1}(\frac{a}{\nu}), & \text{if } x \in \mathcal{S}_{y_1} \setminus \phi^{-1}(\mathcal{S}_{y_0}). \end{cases} \end{aligned}$$

- Consider the case  $0 \in \phi^{-1}(\mathcal{S}_{y_0}) \cap \mathcal{S}_{y_1}$ . It is well-known that for any  $\delta > 0$  there is a  $T > 0$  and a  $u \in W^{1,2}((0, T))$  with  $u(0) = 0$  and  $u(T) = 1$  such that  $\int_0^T |u'|^2 + (1-u)^2 dx < 1 + \delta$ . Let

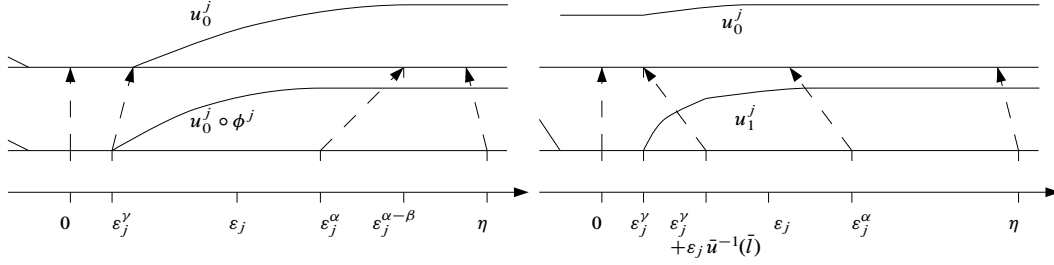


FIG. 9. The deformations (dashed arrows) and phase fields for the cases  $0 \in \phi^{-1}(\mathcal{S}_{y_0}) \setminus \mathcal{S}_{y_1}$  and  $0 \in \mathcal{S}_{y_1} \setminus \phi^{-1}(\mathcal{S}_{y_0})$

$\gamma > 1 > \alpha > 0$  and define

$$u_0^j(x) = u_1^j(x) = \begin{cases} 0, & |x| < \epsilon_j^\gamma, \\ u\left(\frac{|x| - \epsilon_j^\gamma}{\epsilon_j}\right), & \epsilon_j^\gamma \leq |x| \leq \epsilon_j T + \epsilon_j^\gamma, \\ 1, & \epsilon_j T + \epsilon_j^\gamma < |x|, \end{cases}$$

$$\phi^j(x) = \begin{cases} x, & |x| < \epsilon_j^\alpha, \\ \text{sgn}(x)\epsilon_j^\alpha + [\phi(x) - \phi(\text{sgn}(x)\epsilon_j^\alpha)] \frac{\phi(\text{sgn}(x)\eta) - \text{sgn}(x)\epsilon_j^\alpha}{\phi(\text{sgn}(x)\eta) - \phi(\text{sgn}(x)\epsilon_j^\alpha)}, & \epsilon_j^\alpha \leq |x| \leq \eta, \\ \phi(x), & \eta < |x|. \end{cases}$$

For  $y_i^j$  we take the original image  $y_i$ , just smoothed out within  $[-\epsilon_j^\gamma, \epsilon_j^\gamma]$ . It is well-known that for this recovery sequence,

$$\limsup_{j \rightarrow \infty} \mathcal{E}_{\text{AT}, \phi(V_0)}^{\epsilon_j} [y_0^j, u_0^j] + \mathcal{E}_{\text{AT}, V_0}^{\epsilon_j} [y_1^j, u_1^j] \leq \int_{\phi(V_0 \setminus \{0\})} |\nabla y_0|^2 dx + \int_{V_0 \setminus \{0\}} |\nabla y_1|^2 dx + 2\nu(1 + \delta),$$

and by the arbitrariness of  $\delta$  we obtain the desired limit. It remains to show the convergence of the matching and the deformation energy. We have

$$\frac{a}{\epsilon_j} \int_{V_0} (u_0^j \circ \phi^j - u_1^j)^2 dx = \frac{a}{\epsilon_j} \int_{-\epsilon_j^\alpha}^{\epsilon_j^\alpha} (u_0^j \circ \phi^j - u_1^j)^2 dx + \frac{a}{\epsilon_j} \int_{V_0 \setminus [-\epsilon_j^\alpha, \epsilon_j^\alpha]} (u_0^j \circ \phi^j - u_1^j)^2 dx,$$

where the first term is zero and the integrand of the second term becomes  $(1 - 1)^2 = 0$  for  $j$  large enough (since then  $\epsilon_j^\alpha > \epsilon_j T$ ). Also,  $\phi^j \rightharpoonup \phi$  in  $W^{1,p}(V_0)$  and

$$\mathcal{W}_{V_0}[\phi^j] = 2\epsilon_j^\alpha W(1) + \int_{V_0 \setminus [-\epsilon_j^\alpha, \epsilon_j^\alpha]} W\left(\frac{\phi(\text{sgn}(x)\eta) - \text{sgn}(x)\epsilon_j^\alpha}{\phi(\text{sgn}(x)\eta) - \phi(\text{sgn}(x)\epsilon_j^\alpha)} \mathfrak{D}\phi\right) dx$$

of which the first term is zero and the second one converges to  $\mathcal{W}_{V_0}[\phi]$  since its integrand converges pointwise to  $W(\mathfrak{D}\phi)$  (due to the continuity of  $\phi$  and of  $W$ ) and is bounded by some constant plus a multiple of  $W(\mathfrak{D}\phi)$  (due to the growth condition on  $W$ ) so that Lebesgue's theorem can be applied.

- In the case  $0 \in \phi^{-1}(\mathcal{S}_{y_0}) \setminus \mathcal{S}_{y_1}$  we take  $u_0^j$  and  $y_0^j$  as before, but  $u_1^j \equiv 1$  and  $y_1^j = y_1$ . Furthermore, define (see Fig. 9 left)

$$\phi^j(x) = \begin{cases} \varepsilon_j^{-\beta} x, & |x| < \varepsilon_j^\alpha, \\ \operatorname{sgn}(x)\varepsilon_j^{\alpha-\beta} + \left[\phi(x) - \phi(\operatorname{sgn}(x)\varepsilon_j^\alpha)\right] \frac{\phi(\operatorname{sgn}(x)\eta) - \operatorname{sgn}(x)\varepsilon_j^{\alpha-\beta}}{\phi(\operatorname{sgn}(x)\eta) - \phi(\operatorname{sgn}(x)\varepsilon_j^\alpha)}, & \varepsilon_j^\alpha \leq |x| \leq \eta, \\ \phi(x), & \eta < |x|, \end{cases}$$

for some  $\beta$  with  $1 > \alpha > \beta$ ,  $r\beta > 0$  (where  $r$  is the exponent from the growth condition on  $W$ ). Here again, the correct convergence of the Ambrosio–Tortorelli energy terms is standard, and it remains to show the convergence of the matching and the deformation energy. We have

$$\frac{a}{\varepsilon_j} \int_{V_0} (u_0^j \circ \phi^j - u_1^j)^2 dx = \frac{a}{\varepsilon_j} \int_{-\varepsilon_j^\alpha}^{\varepsilon_j^\alpha} (u_0^j \circ \phi^j - 1)^2 dx + \frac{a}{\varepsilon_j} \int_{V_0 \setminus [-\varepsilon_j^\alpha, \varepsilon_j^\alpha]} (u_0^j \circ \phi^j - 1)^2 dx,$$

where for  $j$  large enough, the integrand of the second term becomes  $(1 - 1)^2 = 0$  and the first term becomes (after the change of variables  $x \rightarrow \varepsilon_j^{-\beta} x$ )

$$a\varepsilon_j^{\beta-1} \int_{-\varepsilon_j T - \varepsilon_j^\gamma}^{\varepsilon_j T + \varepsilon_j^\gamma} (u_0^j - 1)^2 dx = 2a\varepsilon_j^{\gamma+\beta-1} + a\varepsilon_j^\beta 2 \int_0^T (u - 1)^2 dx \leq 2a\varepsilon_j^\beta (1 + \delta + \varepsilon_j^{\gamma-1}) \xrightarrow{j \rightarrow \infty} 0.$$

Also,

$$\mathcal{W}_{V_0}[\phi^j] = 2\varepsilon_j^\alpha W(\varepsilon_j^{-\beta}) + \int_{V_0 \setminus [-\varepsilon_j^\alpha, \varepsilon_j^\alpha]} W\left(\frac{\phi(\operatorname{sgn}(x)\eta) - \operatorname{sgn}(x)\varepsilon_j^\alpha}{\phi(\operatorname{sgn}(x)\eta) - \phi(\operatorname{sgn}(x)\varepsilon_j^\alpha)} \mathfrak{D}\phi\right) dx$$

of which the second term converges to  $\mathcal{W}_{V_0}[\phi]$  as before, and the first term is bounded by  $2\varepsilon_j^\alpha(C_1(2\varepsilon_j^{-r\beta} + \varepsilon_j^{r\beta}) + C_2)$ , which converges to zero due to  $\alpha > r\beta$ .

- Finally, if  $0 \in \mathcal{S}_{y_1} \setminus \phi^{-1}(\mathcal{S}_{y_0})$ , let  $\bar{l}$  be the unique minimizer from Lemma 5.7 for  $\kappa = 0$ ,  $\lambda = 1$ , and  $\bar{u}$  the unique minimizer of  $U^{0, \bar{l}, a}$  from Lemma 5.6. We take  $\gamma$  such that  $1 < \gamma < 1 + \frac{1}{r}$  and define (see Fig. 9 right)

$$u_1^j(x) = \begin{cases} 0, & |x| < \varepsilon_j^\gamma, \\ \bar{u}\left(\frac{|x| - \varepsilon_j^\gamma}{\varepsilon_j}\right), & 0 \leq |x| - \varepsilon_j^\gamma < \varepsilon_j \bar{u}^{-1}(\bar{l}), \\ u\left(\frac{|x| - \varepsilon_j^\gamma}{\varepsilon_j} - \bar{u}^{-1}(\bar{l}) + u^{-1}(\bar{l})\right), & 0 \leq |x| - \varepsilon_j^\gamma - \varepsilon_j \bar{u}^{-1}(\bar{l}) \leq \varepsilon_j(T - u^{-1}(\bar{l})), \\ 1, & \text{else,} \end{cases}$$

$$u_0^j(x) = \begin{cases} \bar{l}, & |x| < \varepsilon_j^\gamma, \\ u_1^j(|x| + \varepsilon_j \bar{u}^{-1}(\bar{l})), & |x| \geq \varepsilon_j^\gamma, \end{cases}$$

$$\phi^j(x) = \begin{cases} \frac{\varepsilon_j^\gamma}{\varepsilon_j^\gamma + \varepsilon_j \bar{u}^{-1}(\bar{l})} x, & |x| < \varepsilon_j^\gamma + \varepsilon_j \bar{u}^{-1}(\bar{l}), \\ x \mp \varepsilon_j \bar{u}^{-1}(\bar{l}), & \varepsilon_j^\gamma + \varepsilon_j \bar{u}^{-1}(\bar{l}) \leq \pm x < \varepsilon_j^\alpha, \\ \pm \varepsilon_j^\alpha \pm \varepsilon_j \bar{u}^{-1}(\bar{l}) + \frac{[\phi(x) - \phi(\pm \varepsilon_j^\alpha)][\phi(\pm \eta) \mp (\varepsilon_j^\alpha + \varepsilon_j \bar{u}^{-1}(\bar{l}))]}{\phi(\pm \eta) - \phi(\pm \varepsilon_j^\alpha)}, & \varepsilon_j^\alpha \leq \pm x \leq \eta, \\ \phi(x), & \eta < |x|. \end{cases}$$

Furthermore,  $y_1^j$  is defined as in the case  $0 \in \phi^{-1}(\mathcal{S}_{y_0}) \cap \mathcal{S}_{y_1}$ , and for  $y_0^j$  we take the constant sequence  $y_0$ . The convergence of  $\int_{\phi(-\eta)}^{\phi(\eta)} (u_0^j)^2 |\nabla y_0^j|^2 dx + \int_{-\eta}^{\eta} (u_1^j)^2 |\nabla y_1^j|^2 dx$  against the correct limit follows by Lebesgue's theorem. The matching and length regularization terms can then be written as

$$\begin{aligned} \frac{a}{\varepsilon_j} \int_{-\eta}^{\eta} |u_0^j \circ \phi^j - u_1^j|^2 dx &= \frac{a}{\varepsilon_j} \int_{-\varepsilon_j^\gamma - \varepsilon_j \bar{u}^{-1}(\bar{l})}^{\varepsilon_j^\gamma + \varepsilon_j \bar{u}^{-1}(\bar{l})} |\bar{l} - u_1^j|^2 dx \\ &= 2a \int_0^{\varepsilon_j^{\gamma-1} + \bar{u}^{-1}(\bar{l})} |\bar{l} - u_1^j(\varepsilon_j x)|^2 dx \xrightarrow{j \rightarrow \infty} 2a \int_0^{\bar{u}^{-1}(\bar{l})} |\bar{l} - \bar{u}|^2 dx, \\ \frac{\nu}{2} \int_{\phi(-\eta)}^{\phi(\eta)} \varepsilon_j |\nabla u_0^j|^2 + \frac{1}{\varepsilon_j} (1 - u_0^j)^2 dx &= \nu \varepsilon_j^{\gamma-1} (1 - \bar{l})^2 + \nu \int_{u^{-1}(\bar{l})}^T |u'|^2 + (1 - u)^2 dx \xrightarrow{j \rightarrow \infty} 2\nu \int_{\bar{l}}^1 1 - z dz + O(\delta), \\ \frac{\nu}{2} \int_{-\eta}^{\eta} \varepsilon_j |\nabla u_1^j|^2 + \frac{1}{\varepsilon_j} (1 - u_1^j)^2 dx &= \nu \varepsilon_j^{\gamma-1} + \nu \int_0^{\bar{u}^{-1}(\bar{l})} |\bar{u}'|^2 + (1 - \bar{u})^2 dx \\ + \nu \int_{u^{-1}(\bar{l})}^T |u'|^2 + (1 - u)^2 dx &\xrightarrow{j \rightarrow \infty} \nu \int_0^{\bar{u}^{-1}(\bar{l})} |\bar{u}'|^2 + (1 - \bar{u})^2 dx + 2\nu \int_{\bar{l}}^1 1 - z dz + O(\delta). \end{aligned}$$

Hence, up to  $O(\delta)$ , the sum of the three terms converges to  $\nu Z^{0,1}(\frac{a}{\nu}) + \nu$  by Lemma 5.7, and by the arbitrariness of  $\delta$  we obtain the desired convergence. Concerning the deformation energy,

$$\begin{aligned} \mathcal{W}_{V_0}[\phi^j] &= 2(\varepsilon_j^\gamma + \varepsilon_j \bar{u}^{-1}(\bar{l})) W\left(\frac{\varepsilon_j^\gamma}{\varepsilon_j^\gamma + \varepsilon_j \bar{u}^{-1}(\bar{l})}\right) + 2(\varepsilon_j^\alpha - \varepsilon_j^\gamma - \varepsilon_j \bar{u}^{-1}(\bar{l})) W(1) \\ &\quad + \int_{V_0 \setminus [-\varepsilon_j^\alpha, \varepsilon_j^\alpha]} W\left(\frac{\phi(\operatorname{sgn}(x)\eta) - \operatorname{sgn}(x)(\varepsilon_j^\alpha + \varepsilon_j \bar{u}^{-1}(\bar{l}))}{\phi(\operatorname{sgn}(x)\eta) - \phi(\operatorname{sgn}(x)\varepsilon_j^\alpha)} \mathfrak{D}\phi\right) dx, \end{aligned}$$

where the first two terms converge to zero (due to the bound on  $W$  and  $\gamma < 1 + \frac{1}{r}$ ) and the last one converges to  $\mathcal{W}_{V_0}[\phi]$  as before.  $\square$

**Remark 5.8** *Instead of requiring the upper bound  $W(A) \leq C_1(\|A\|^r + \det A^r + \det A^{-r}) + C_2$ , one can prove the result also for a more general (poly-)convex bound  $W(A) \leq \Gamma(\det A) + F(\|A\|)$  by adapting the scales  $[-\varepsilon^\alpha, \varepsilon^\alpha]$  within which the deformation is changed.*

#### 5.4 Proof of Theorem 4.6

Due to the arguments from the previous sections, it seems reasonable to increase the rate at which the weight of the fitting term tends to infinity as  $\varepsilon \rightarrow 0$ . If this rate is large enough, the matching deformation can no longer squeeze the phase field  $u_0$  to make the mismatch energy vanish. In the limit this would forbid any mismatch between  $u_0 \circ \phi$  and  $u_1$  so that both develop full ghost phase fields and thus encode the same edges. Thm. 4.6 provides information on the needed rate of increase.

Since the proof employs exactly the same techniques as in the previous sections, we only provide its outline, pointing out and explaining the small differences to the previous section along the way.

*Outline of proof for Thm. 4.6.* For the lim inf-inequality, as usual let  $\varepsilon_j \rightarrow 0$  and  $(y_0^j, y_1^j, u_0^j, u_1^j, \phi^j) \rightarrow (y_0, y_1, u_0, u_1, \phi)$  be given with the same properties as in the proof of Thm. 4.5. For  $t \in (1, \frac{r}{r-1})$  the proof of Thm. 4.5 can be copied, hence we only consider the case  $t \in (\frac{p}{p-1}, \infty)$  for which all arguments can be repeated except for the lim inf-inequality of

$$E^j[u_0^j, u_1^j, \phi^j] = \frac{a}{\varepsilon_j^t} \mathfrak{F}_{U_\eta}[u_0^j, u_1^j, \phi^j] + \nu \mathfrak{L}_{\text{AT}, \phi(U_\eta)}^{\varepsilon_j}[u_0^j] + \nu \mathfrak{L}_{\text{AT}, U_\eta}^{\varepsilon_j}[u_1^j],$$

where  $U_\eta = B_\eta(\phi^{-1}(\mathcal{S}_{y_0}) \setminus \mathcal{S}_{y_1})$  and  $\eta$  is small enough so that  $\overline{U_\eta}$  contains no element of  $\mathcal{S}_{y_1}$ . For simplicity we may assume  $U_\eta$  to be a single interval with just one single element  $\phi^{-1}(x_c) \in \phi^{-1}(\mathcal{S}_{y_0})$  (otherwise split  $U_\eta$  into several intervals and consider each separately).

We now intend to show  $\inf_{x \in U_\eta} u_1^j(x) \rightarrow_{j \rightarrow \infty} 0$ . Together with  $u_1^j \rightarrow 1$  almost everywhere this implies via the standard Ambrosio–Tortorelli argument that  $\mathfrak{L}_{\text{AT}, U_\eta}^{\varepsilon_j}[u_1^j]$  converges against something greater than or equal to 1. Since the same holds for  $\mathfrak{L}_{\text{AT}, \phi(U_\eta)}^{\varepsilon_j}[u_0^j]$ , this is the required lim inf-inequality. We proceed in steps.

1. For a contradiction, assume  $\inf_{x \in U_\eta} u_1^j(x)$  to be uniformly bounded below by  $\bar{l} > 0$ .
2. From the standard Ambrosio–Tortorelli argument we know  $u_0^j(x_c^j) \rightarrow 0$  for a sequence  $x_c^j \rightarrow x_c$  in  $\phi(U_\eta)$ . We now show  $u_0^j \leq \bar{u}_0^j$  for all  $j$  with

$$\bar{u}_0^j(x) = \min\{1, u_0^j(x_c^j) + C\sqrt{|x - x_c^j|/\varepsilon_j}\}$$

for some  $C > 0$ . Indeed, for any  $\delta > 0$  we have

$$\text{vol}\left(\left\{|(u_0^j)'| \geq \frac{1}{\delta}\right\}\right) \leq \frac{\delta^2}{\nu \varepsilon_j} \mathfrak{g}_{\text{edge}}^{t, \varepsilon_j}[y_0^j, y_1^j, u_0^j, u_1^j, \phi^j] \leq \tilde{C} \frac{\delta^2}{\varepsilon_j}$$

for some  $\tilde{C} > 0$ . Thus,  $u_0^j(x) = u_0^j(x_c^j) + \int_{x_c^j}^x (u_0^j)'(x) dx \leq u_0^j(x_c^j) + \int_0^{|x-x_c^j|} \sqrt{\tilde{C}/(\varepsilon_j z)} dz$ , which implies the desired statement.

3. Likewise,  $|\phi^j(x) - x_c^j| \leq |\bar{\phi}^j(x) - x_c^j|$  with

$$\bar{\phi}^j(x) = x_c^j + \tilde{C} \text{sgn}(x - (\phi^j)^{-1}(x_c^j)) |x - (\phi^j)^{-1}(x_c^j)|^{1-\frac{1}{p}}$$

for some  $\tilde{C} > 0$ . Indeed, for any  $\delta > 0$  small enough we have

$$\text{vol}\left(\left\{|(\phi^j)'| \geq \frac{1}{\delta}\right\}\right) \leq \delta^p \tilde{C} \mathfrak{g}_{\text{edge}}^{t, \varepsilon_j}[y_0^j, y_1^j, u_0^j, u_1^j, \phi^j] \leq \hat{C} \delta^p$$

for some  $\tilde{C}, \hat{C} > 0$  so that the claim follows by the same argument as above.

4. We now show that the matching term in  $E^j$  is decreased if on  $I^j = (\bar{u}^j)^{-1}([0, \bar{l}])$  we replace  $u_0^j$  by  $\bar{u}_0^j$  and on  $(\phi^j)^{-1}(I^j)$  we replace  $\phi^j$  and  $u_1^j$  by  $\bar{\phi}^j$  and  $\bar{u}_1^j = \bar{l}$ . This indeed follows from

$$u_0^j \circ \phi^j \leq \bar{u}_0^j \circ \phi^j \leq \bar{u}_0^j \circ \bar{\phi}^j \leq \bar{u}_1^j \leq u_1^j$$

on  $(\phi^j)^{-1}(I^j)$ , where the second inequality results from the monotonicity of  $\bar{u}_0^j$  on either side of  $x_c^j$ .

5. Finally, although the value of the matching term has been decreased, it still diverges to  $\infty$  as  $j \rightarrow \infty$ , contradicting the assumption of a uniformly bounded  $\mathfrak{G}_{\text{edge}}^{t, \varepsilon_j}[y_0^j, y_1^j, u_0^j, u_1^j, \phi^j]$  and thus concluding the proof. Indeed,

$$\begin{aligned} \frac{a}{\varepsilon_j^t} \int_{U_n} (u_0^j \circ \phi^j - u_1^j)^2 dx &\geq \frac{a}{\varepsilon_j^t} \int_{(\phi^j)^{-1}(I^j)} (\bar{u}_0^j \circ \bar{\phi}^j - \bar{u}_1^j)^2 dx \\ &\geq 2 \frac{a}{\varepsilon_j^t} \int_0^{\left(\frac{l^2 \varepsilon_j}{C^2 \tilde{C}}\right)^{\frac{p}{p-1}}} \left(C \sqrt{\tilde{C} x^{1-\frac{1}{p}} / \varepsilon_j} - \bar{l}\right)^2 dx \\ &= 2a(C^2 \tilde{C})^{\frac{p}{p-1}} \frac{(p-1)^2}{(3p-1)(2p-1)} \bar{l}^{-\frac{4p-2}{p-1}} \varepsilon_j^{\frac{p}{p-1}-t} \xrightarrow{j \rightarrow \infty} \infty. \end{aligned}$$

Concerning the lim sup-inequality, for  $t > \frac{p}{p-1}$  the proof proceeds exactly as in Thm. 4.5, only that in the four different cases we this time take exactly the same recovery sequence, namely the one which originally belonged to points in  $\phi^{-1}(\mathcal{S}_{y_0}) \cap \mathcal{S}_{y_1}$ . For  $t < \frac{r}{r-1}$  we proceed as in Thm. 4.5 with only two differences: First, the recovery sequence around points in  $\mathcal{S}_{y_1} \setminus \phi^{-1}(\mathcal{S}_{y_0})$  is taken to be the same as around points in  $\phi^{-1}(\mathcal{S}_{y_0}) \cap \mathcal{S}_{y_1}$ . Second, the recovery sequence around points in  $\phi^{-1}(\mathcal{S}_{y_0}) \setminus \mathcal{S}_{y_1}$  is a little bit more elaborate.  $y_0^j, y_1^j, u_0^j, u_1^j$  are chosen as in Thm. 4.5, but  $\phi^j$  on the interval  $[-\varepsilon_j^\alpha, \varepsilon_j^\alpha]$  shall be given by  $\phi^j(x) = x^b$  for some  $b$  with  $t < \frac{1}{b} < \frac{r}{r-1}$ . The desired convergence of all terms can then readily be shown, in particular the mismatch term behaves for large  $j$  like  $\frac{a}{\varepsilon_j^t} \varepsilon_j^{\frac{1}{b}} \rightarrow_{j \rightarrow \infty} 0$ .  $\square$

### 5.5 Proof of Theorem 4.7

In contrast to the previous models, this model does not contain a phase field matching term and thus does not exhibit an alteration of the phase field profile by the deformation. As a result, the  $\Gamma$ -convergence proof is much simpler and does not require any essentially new ideas. Indeed, both the lim inf- and lim sup-inequality are just slight adaptations of the standard argument for the Ambrosio–Tortorelli functional in [8, Thm. 8.1].

*Proof of Theorem 4.7.* As in the earlier proofs, for the lim inf-inequality the fidelity terms  $\int_{\Omega} (y_i - \hat{y}_i)^2 dx$  may be neglected as continuous perturbations, and we may restrict ourselves to sequences  $\varepsilon_j \rightarrow 0$  and  $(y_0^j, y_1^j, u_0^j, \phi^j) \rightarrow (y_0, y_1, u_0, \phi)$  in  $(L^1(\Omega))^3 \times w\text{-}W_{\text{id}}^{1,p}(\Omega)$  such that  $y_0^j, y_1^j, u_0^j, \phi^j$  also converge pointwise and satisfy  $0 \leq u_0^j \leq 1$  and that the limit  $\lim_{j \rightarrow \infty} \tilde{\mathfrak{G}}_{\text{edge}}^{\varepsilon_j}[y_0^j, y_1^j, u_0^j, \phi^j]$  exists and is finite so that  $u_0 = 1$  a. e. and the  $\phi^j$  as well as  $\phi$  are homeomorphisms.

By the conditions on  $W$  we have  $\liminf_{j \rightarrow \infty} \mathcal{W}[\phi^j] \geq \mathcal{W}[\phi]$ . For the remaining terms we follow the standard argument for the Ambrosio–Tortorelli segmentation [8, Thm. 8.1]: We may assume the existence of a finite set  $\mathcal{S} \subset \Omega$  such that on every open  $I \subset \subset \Omega \setminus \mathcal{S}$  we have  $\frac{1}{2} < u_0^j < \frac{3}{2}$  for  $j$  large enough, which implies  $y_0^j \rightarrow y_0$  in  $W^{1,2}(I)$  and  $y_1^j \rightarrow y_1$  in  $W^{1,2}(\phi^{-1}(I))$  (where we have used the convergence  $\phi^j \rightarrow \phi$  in  $C^0(\bar{\Omega})$  due to Hölder embedding). Since  $I$  is arbitrary and

$\phi$  is homeomorphic, we obtain  $\phi(\mathcal{S}_{y_1}) \cup \mathcal{S}_{y_0} \subset \mathcal{S}$  and by the standard argument

$$\begin{aligned} & \liminf_{j \rightarrow \infty} \int_{\Omega} ((u_0^j)^2 + k_{\varepsilon_j}) |\nabla y_0^j|^2 dx + a \int_{\Omega} ((u_0^j \circ \phi^j)^2 + k_{\varepsilon_j}) |\nabla y_1^j|^2 dx \\ & \geq \int_{\Omega \setminus \mathcal{S}} |\nabla y_0|^2 dx + a \int_{\Omega \setminus \phi^{-1}(\mathcal{S})} |\nabla y_1|^2 dx = \int_{\Omega \setminus \mathcal{S}_{y_0}} |\nabla y_0|^2 dx + a \int_{\Omega \setminus \mathcal{S}_{y_1}} |\nabla y_1|^2 dx. \end{aligned}$$

Furthermore, the standard argument also implies that  $\inf_{x \in U} u_0^j(x)$  tends to zero for any neighborhood  $U$  of any point  $x \in \mathcal{S}$ , which in turn implies  $\liminf_{j \rightarrow \infty} \mathfrak{L}_{AT}^{\varepsilon_j}[u_0^j] \geq \mathcal{H}^{d-1}(\mathcal{S}_{y_0} \cup \phi(\mathcal{S}_{y_1}))$ . This completes the proof of the lim inf-inequality.

For the recovery sequence, as in the proof of Thm. 4.5 it suffices to consider the case  $\Omega = (-\eta, \eta)$  for some  $\eta > 0$  and  $\mathcal{S}_{y_0} \cup \phi(\mathcal{S}_{y_1}) = \{0\}$  (where additionally we have to ensure that the elements  $y_0^j, y_1^j, u_0^j, \phi^j$  of the recovery sequence are compatible with  $y_0, y_1, u_0, \phi$  at  $\{-\eta, \eta\}$ ).

We may assume  $u_0 \equiv 1$ , since otherwise there is nothing to prove. Let  $\xi_\varepsilon = o(\varepsilon)$  such that also  $\phi(\phi^{-1}(0) + \xi_\varepsilon) - \phi(\phi^{-1}(0) - \xi_\varepsilon) = o(\varepsilon)$ . As in the proof of Thm. 4.5 we use that for any  $\delta > 0$  there is a  $T > 0$  and a  $u \in W^{1,2}((0, T))$  with  $u(0) = 0$  and  $u(T) = 1$  such that  $\int_0^T |u'|^2 + (1-u)^2 dx < 1 + \delta$ . We define

$$u_0^j(x) = \begin{cases} 0, & |x| < \xi_{\varepsilon_j}, \\ u\left(\frac{|x| - \xi_{\varepsilon_j}}{\varepsilon_j}\right), & \xi_{\varepsilon_j} \leq |x| \leq \varepsilon_j T + \xi_{\varepsilon_j}, \\ 1, & \varepsilon_j T + \xi_{\varepsilon_j} < |x|. \end{cases}$$

Furthermore, we choose  $\phi^j = \phi$  and  $y_i^j$  to equal  $y_i$ ,  $i = 0, 1$ , except on  $[-\xi_{\varepsilon_j}, \xi_{\varepsilon_j}]$ , where  $y_0$  is smoothed, and on  $[\phi^{-1}(0) - \xi_{\varepsilon_j}, \phi^{-1}(0) + \xi_{\varepsilon_j}]$ , where  $y_1$  is smoothed. For this sequence, it is well-known that

$$\begin{aligned} \lim_{j \rightarrow \infty} \tilde{\mathfrak{J}}_{\text{edge}}^{\varepsilon_j}[y_0^j, y_1^j, u_0^j, \phi^j] & \leq \alpha \int_{\Omega} |y_0 - \hat{y}_0|^2 dx + \int_{\Omega \setminus \mathcal{S}_{y_0}} |\nabla y_0|^2 dx + \nu(1 + \delta) \\ & \quad + \alpha \int_{\Omega} |y_1 - \hat{y}_1|^2 dx + a \int_{\Omega \setminus \mathcal{S}_{y_1}} |\nabla y_1|^2 dx + \mathcal{W}[\phi] \end{aligned}$$

which by the arbitrariness of  $\delta$  concludes the proof. □

### 5.6 The higher-dimensional case and why tangential displacements matter

In higher dimensions, the situation for joint edge segmentation and registration becomes more complicated than in 1D, which is associated with the possibility of tangential deformations along the image edges. For illustration, consider the functional  $\mathfrak{J}_{\text{edge}}^\varepsilon$  from Thm. 4.5. Again, in the  $\Gamma$ -limit we expect only to see a contribution to the mismatch energy from the edges  $\mathcal{S}_{y_1} \setminus \phi^{-1}(\mathcal{S}_{y_0})$  since the phase fields belonging to edges  $\phi^{-1}(\mathcal{S}_{y_0}) \setminus \mathcal{S}_{y_1}$  will be compressed in normal direction so that they vanish in the limit (cf. the proof of Thm. 4.5). As in 1D, the weight of the asymmetric mismatch in the limit will be smaller than  $a$  due to the appearance of ghost edges in the phase field function  $u_0$  at places where the phase field  $u_1$  encodes an edge. These ghost edges reduce the mismatch energy, but at the same time they contribute to the total energy with additional length energy  $\nu \mathfrak{L}_{AT}^\varepsilon[u_0]$ . Balancing both contributions results in optimal ghost field profiles and in 1D produces the mismatch

weight  $\nu Z^{0,1}(\frac{a}{\nu})$ . In higher dimensions, the mismatch weight should not only depend on  $\nu$  and  $a$ , but also on the deformation tangential to the edges: If the edges  $\mathcal{S}_{y_1} \setminus \phi^{-1}(\mathcal{S}_{y_0})$  are shortened by the deformation  $\phi$ , then the length energy  $\nu \mathcal{L}_{\text{AT}}^\varepsilon[u_0]$  plays a smaller role than if the edges are elongated so that the optimal balance between length and mismatch energy (and thus the optimal ghost edge profile) should depend on the local edge length change,  $|\text{cof}(\mathfrak{D}\phi)n_{\mathcal{S}_{y_1}}|$  (where  $n_{\mathcal{S}_{y_1}}$  is the normal to the image edges  $\mathcal{S}_{y_1}$ ). In more detail, if the ghost edges along  $\phi(\mathcal{S}_{y_1}) \setminus \mathcal{S}_{y_0}$  are very long, then they will be not very pronounced so as to keep  $\nu \mathcal{L}_{\text{AT}}^\varepsilon[u_0]$  small, whereas if the ghost edges are very short so that  $\nu \mathcal{L}_{\text{AT}}^\varepsilon[u_0]$  is small anyway, then they will be very pronounced so as to make the mismatch  $\frac{a}{\varepsilon} \mathcal{F}[u_0, u_1, \phi]$  small.

Recalling the proofs of Thm. 4.5 and the associated Lemma 5.7, the ghost edge length energy  $\mathcal{L}_{\text{AT}}^\varepsilon[u_0]$  corresponds to half of the second term in the definition of  $V^{\kappa, \lambda, a}[l]$  in Lemma 5.7. Hence, one might expect the weight of the mismatch penalty in the limit to be given locally by a function of the form

$$\nu Z^{0,1}(\frac{a}{\nu}, |\text{cof}(\mathfrak{D}\phi)n_{\mathcal{S}_{y_1}}|) = \min_{l \in [0,1]} \nu \bar{U}^{0,1, \frac{a}{\nu}}[l] + \nu(2 + 2|\text{cof}(\mathfrak{D}\phi)n_{\mathcal{S}_{y_1}}|) \int_l^1 1 - z \, dz - 1.$$

$Z^{0,1}(a, b)$  is obviously monotonically increasing in  $a$  and  $b$  with  $Z^{0,1}(0, b) = 0$ ,  $\lim_{a \rightarrow \infty} Z^{0,1}(a, b) = b$ ,  $Z^{0,1}(a, 0) = 0$ ,  $Z^{0,1}(a, 1) = Z^{0,1}(a)$ , and  $\lim_{b \rightarrow \infty} Z^{0,1}(a, b) = a$  as well as  $\frac{\partial}{\partial a} Z^{0,1}(a, b)|_{a=0} = 1$  (which can be computed just as in Sec. 5.3). The expected mismatch term in the  $\Gamma$ -limit would then be given by a term like

$$\int_{\mathcal{S}_{y_1} \setminus \phi^{-1}(\mathcal{S}_{y_0})} \nu Z^{0,1}(\frac{a}{\nu}, |\text{cof}(\mathfrak{D}\phi)n_{\mathcal{S}_{y_1}}|) \, d\mathcal{H}^{d-1}.$$

However, since  $Z^{0,1}(a, b)$  is concave in  $b$ , this term is not weakly lower semi-continuous in  $\phi \in W^{1,p}(\Omega)$  (and therefore cannot be the  $\Gamma$ -limit), and we thus expect oscillations of the deformation tangentially to the edges. Indeed, this behavior is observed in the proof of Example 4.8 below.

Note that by modifying the functional and increasing the rate at which the weight of the mismatch term tends to infinity as  $\varepsilon \rightarrow 0$ , the mismatch term would at some point begin to cost too much even with oscillating deformations so that  $u_0$  would develop a full ghost phase field, resulting in the mismatch penalty  $\nu \mathcal{H}^{d-1}(\phi(\mathcal{S}_{y_1}) \setminus \mathcal{S}_{y_0})$ . This is consistent with the observation that  $\lim_{a \rightarrow \infty} Z^{0,1}(a, \cdot)$  is convex so that the weak lower semi-continuity of  $\int_{\mathcal{S}_{y_1} \setminus \phi^{-1}(\mathcal{S}_{y_0})} \nu Z^{0,1}(\infty, |\text{cof}(\mathfrak{D}\phi)n_{\mathcal{S}_{y_1}}|) \, d\mathcal{H}^{d-1} = \nu \mathcal{H}^{d-1}(\phi(\mathcal{S}_{y_1}) \setminus \mathcal{S}_{y_0})$  is satisfied.

If instead the deformation energy  $\mathcal{W}[\phi]$  would be made to depend also on the Hessian or higher derivatives of  $\phi$ , the  $\Gamma$ -limit would be considered using some weak  $W^{n,p}(\Omega)$ -topology, and for sufficiently large  $p$  and  $n$  one would obtain strong convergence in the dilation factor  $\text{cof} \mathfrak{D}\phi$  so that the above-mentioned oscillation of tangential deformations is prohibited ( $n = 3$  suffices to obtain strong convergence of the trace of  $\text{cof} \mathfrak{D}\phi$  on the edge set  $\mathcal{S}_{y_1} \setminus \phi^{-1}(\mathcal{S}_{y_0})$ ; possibly even  $n = 2$  is sufficient to prevent oscillations). The concavity of  $Z^{0,1}(a, \cdot)$  then no longer poses a problem to the functional's lower semi-continuity, and one can expect the above-proposed mismatch term to appear in the limit.

*Proof of Example 4.8.* The lim inf-inequality is trivial due to the weak lower semi-continuity of  $\mathcal{W}$  and the classical result by Ambrosio and Tortorelli (note that the matching term is simply disregarded for the lim inf-inequality).

For a recovery sequence (given a sequence  $\varepsilon_j \rightarrow 0$ ), choose  $\frac{\max\{p,r,s\}}{1+\max\{p,r,s\}} < \beta < \alpha < 1$  as well as  $1 > \delta > (1 - \frac{1}{p})\beta$  and  $\delta + 1 - \beta < \gamma < \delta + \frac{\beta}{\max\{p,r,s\}}$ . For  $y_0^j$  and  $y_1^j$  we choose the constant sequence. Furthermore, denoting the optimal Ambrosio–Tortorelli profile by  $u(t) = 1 - \exp(-|t|)$ , we define

$$u_1^j(x_1, x_2) = u(|x_1|/\varepsilon_j).$$

Now let us define the set  $\mathbf{S}^j$  as shown in Fig. 10. It is the union of  $\varepsilon_j^\gamma$  long segments on the  $x_2$ -axis with distance  $\varepsilon_j^\delta$  to each other. We define

$$u_0^j(x) = u(d_{\mathbf{S}^j}(x)/\varepsilon_j),$$

where  $d_{\mathbf{S}^j}$  denotes the distance function to  $\mathbf{S}^j$ . Clearly,  $u_0^j$  and  $u_1^j$  converge to  $1 = u_0 = u_1$  in  $L^1(\Omega)$ . Finally, the deformation  $\phi^j$  is defined as sketched in Fig. 10: For  $|x_1| > \varepsilon_j^\beta$  we have  $\phi^j = \text{id}$ , and for  $|x_1| < \varepsilon_j^\beta$  we have an alternation between uniform compression and uniform dilation in  $x_2$ -direction, while the  $x_1$  coordinate of each point stays unchanged during the deformation. Obviously,  $\phi^j$  weakly converges against the macroscopic displacement  $\phi = \text{id}$ .

Now let us consider the convergence of the single energy terms. The convergence of  $\mathfrak{E}_{\text{AT}}^{\hat{y}_1, \varepsilon_j}[y_1^j, u_1^j]$  is the classical result by Ambrosio and Tortorelli, and the convergence of  $\alpha \int_\Omega (y_0^j - \hat{y}_0)^2 dx + \int_\Omega ((u_0^j)^2 + k_{\varepsilon_j}) |\nabla y_0^j|^2 dx$  is also obvious. Furthermore,

$$\mathfrak{L}_{\text{AT}}^\varepsilon[u_0^j] \leq \varepsilon_j^{-\delta} \left[ \varepsilon_j^\gamma + 2\pi \int_0^\infty R \left( \varepsilon_j \left| \frac{u'(R/\varepsilon_j)}{\varepsilon_j} \right|^2 + \frac{1}{\varepsilon_j} (1-u(R/\varepsilon_j))^2 \right) dR \right] = \varepsilon_j^{\gamma-\delta} + \pi \varepsilon_j^{1-\delta} \xrightarrow{j \rightarrow \infty} 0,$$

where  $\varepsilon_j^{-\delta}$  is (a little larger than) the number of segments of  $\mathbf{S}^j$  and the integral in polar coordinates is larger than the energy contribution around the ends of each segment. The matching energy only has contributions outside  $\{|x_1| < \varepsilon_j^\beta\}$  (which converge to zero due to  $\beta < 1$ ) and inside the regions where  $\phi^j$  is dilating (with  $\frac{a}{\varepsilon_j} \mathfrak{F}[u_0^j, u_1^j, \phi^j] \leq \frac{a}{\varepsilon_j} \varepsilon_j^{-\delta} (\varepsilon_j^\beta \varepsilon_j^\gamma) \rightarrow 0$ ). Finally, the deformation gradient

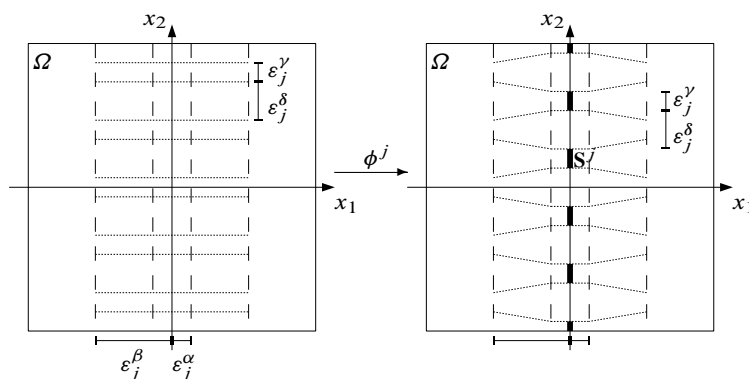


FIG. 10. Sketch of a deformation from the recovery sequence. The set  $\mathbf{S}^j$  consists of the bold lines. The deformation is visualized by the transformation of the dotted horizontal lines between the left and right graph.

on  $\{|x_1| < \varepsilon_j^\beta\}$  is given by

$$\mathfrak{D}\phi^j = \begin{pmatrix} 1 & 0 \\ \partial_{x_1}\phi_2^j & \partial_{x_2}\phi_2^j \end{pmatrix},$$

where  $\partial_{x_2}\phi_2^j$  is an  $x_1$ -dependent convex combination between 1 and  $\varepsilon_j^{\pm(\gamma-\delta)}$  (the sign of the exponent depends on whether we are in a compression or dilation region), and where  $|\partial_{x_1}\phi_2^j|$  is bounded by  $\frac{\varepsilon_j^\delta - \varepsilon_j^\gamma}{2(\varepsilon_j^\beta - \varepsilon_j^\alpha)}$ . Hence the total deformation energy can be bounded by

$$\mathcal{W}[\phi^j] \leq \varepsilon_j^\beta C \left( \max \left\{ 1, \varepsilon_j^{\pm(\gamma-\delta)}, \frac{\varepsilon_j^\delta - \varepsilon_j^\gamma}{2(\varepsilon_j^\beta - \varepsilon_j^\alpha)} \right\} + \varepsilon_j^{r(\gamma-\delta)} + \varepsilon_j^{-s(\gamma-\delta)} + \varepsilon_j^{r(\delta-\gamma)} + \varepsilon_j^{-s(\delta-\gamma)} \right) \xrightarrow{j \rightarrow \infty} 0,$$

where  $C$  is a constant. □

Of course, the particular type of elastic energy density is not relevant to the phenomenon, and we only chose a typical representative for simplicity. Hence, we may expect the  $\Gamma$ -limit of  $\mathfrak{J}_{\text{edge}}^\varepsilon$  for  $\varepsilon \rightarrow 0$  to be just the sum of the elastic energy and the Mumford–Shah segmentation energy for both images—the matching term will disappear. Consequently, in the  $\Gamma$ -limit, the segmentation and deformation energies are completely decoupled, and the energy is no longer a registration energy.

*Acknowledgements.* I warmly thank Martin Rumpf for helpful discussions on the presentation of the material. The research was supported by the Alfred Krupp Prize for Young University Teachers awarded by the Alfred Krupp von Bohlen und Halbach-Stiftung.

## References

1. Ambrosio, L., Fusco, N. & Pallara, D., *Functions of bounded variation and free discontinuity problems*. Oxford Mathematical Monographs. Oxford University Press, New York, 2000. [Zbl0957.49001](#) [MR1857292](#)
2. Ambrosio, L. & Tortorelli, V.M., Approximation of functionals depending on jumps by elliptic functionals via  $\Gamma$ -convergence. *Communications on Pure and Applied Mathematics* **43** (1990), 999–1036. [Zbl10722.49020](#) [MR1075076](#)
3. Ambrosio, L. & Tortorelli, V.M., On the approximation of free discontinuity problems. *Bollettino dell'Unione Matematica Italiana, Sezione B* **6** (1992), 105–123. [Zbl10776.49029](#) [MR1164940](#)
4. Bach Cuadra, M., Duay, V. & Thiran, J.-Ph., Atlas-based segmentation. In Nikos Paragios, James Duncan, and Nicholas Ayache, editors, *Handbook of Biomedical Imaging*, pages 221–244. Springer US, 2015.
5. Ball, J. M., Global invertibility of Sobolev functions and the interpenetration of matter. *Proceedings of the Royal Society of Edinburgh* **88A** (1981), 315–328. [Zbl10478.46032](#) [MR0616782](#)
6. Bhatia, K. K., Hajnal, J. V., Hammers, A. & Rueckert, D., Similarity metrics for groupwise non-rigid registration. In N. Ayache, S. Ourselin, and A. Maeder, editors, *Medical Image Computing and Computer-Assisted Intervention, MICCAI 2007*, volume 4792 of *LNCS*, pages 544–552, 2007.
7. Blume, M., Martinez-Moller, A., Keil, A., Navab, N. & Rafecas, M., Joint reconstruction of image and motion in gated positron emission tomography. *IEEE Transactions on Medical Imaging* **29** (2010), 1892–1906.
8. Braides, A.,  *$\Gamma$ -Convergence for Beginners*. Oxford University Press, Oxford, 2002. [Zbl1198.49001](#) [MR1968440](#)

9. Bresson, X., Esedoğlu, S., Vandergheynst, P., Thiran, J. & Osher, S., Fast global minimization of the active contour/snake model. *Journal of Mathematical Imaging and Vision* **28** (2007), 151–167. [MR2362922](#)
10. Bro-Nielsen, M. & Gramkow, C., Fast fluid registration of medical images. In K. H. Höhne and R. Kikinis, editors, *Visualization in Biomedical Computing: 4th International Conference, VBC*, volume 1131 of *LNCS*, pages 267–276, 1996.
11. Brune, C., Maurer, H. & Wagner, M., Detection of intensity and motion edges within optical flow via multidimensional control. *SIAM Journal on Imaging Sciences* **2** (2009), 1190–1210. [Zb11181.49029](#) [MR2559164](#)
12. Burger, M., Modersitzki, J. & Ruthotto, L., A hyperelastic regularization energy for image registration. *SIAM Journal on Scientific Computing* **35** (2013), B132–B148. [Zb11318.92028](#) [MR3033063](#)
13. Chambolle, A., Cremers, D. & Pock, T., A convex approach to minimal partitions. *SIAM Journal on Imaging Sciences* **5** (2012), 1113–1158. [Zb11256.49040](#) [MR3022190](#)
14. Chan, T. F. & Vese, L. A., Image segmentation using level sets and the piecewise-constant Mumford–Shah model. Technical report, UCLA CAM report 00–14, 2000.
15. Christensen, G. E., Joshi, S. C. & Miller, M. I., Volumetric transformations of brain anatomy. *IEEE Transactions on Medical Imaging* **16** (1997), 864–877.
16. Christensen, G. E., Rabbitt, R. D. & Miller, M. I., Deformable templates using large deformation kinematics. *IEEE Transactions on Image Processing* **5** (1996), 1435–1447.
17. Christensen, G. E., Rabbitt, R. D. & Miller, M. I., A deformable neuroanatomy textbook based on viscous fluid mechanics. In J. Prince and T. Runolfsson, editors, *Proceedings of the 27th Annual Conference on Information Science and Systems*, pages 211–216, 1993.
18. Christensen, G. E., Rabbitt, R. D. & Miller, M. I., 3D brain mapping using a deformable neuroanatomy. *Physics in Medicine and Biology* **39** (1994), 609–618.
19. Droske, M. & Ring, W., A Mumford–Shah level-set approach for geometric image registration. *SIAM Journal on Applied Mathematics* **66** (2006), 2127–2148. [Zb11112.49029](#) [MR2262967](#)
20. Droske, M. & Rumpf, M., A variational approach to non-rigid morphological registration. *SIAM Journal on Applied Mathematics* **64** (2004), 668–687. [Zb11063.49013](#) [MR2049668](#)
21. M. Droske and M. Rumpf, Multi scale joint segmentation and registration of image morphology. *IEEE Transaction on Pattern Recognition and Machine Intelligence*, 29(12):2181–2194, 2007.
22. Gorthi, S., Duay, V., Bresson, X., Bach Cuadra, M., Sánchez Castro, F. J., Pollo, C., Allal, A. S. & Thiran, J.-P., Active deformation fields: Dense deformation field estimation for atlas-based segmentation using the active contour framework. *Medical Image Analysis* **15** (2011), 787–800.
23. Han, J., Berkels, B., Droske, M., Hornegger, J., Rumpf, M., Schaller, C., Scorzin, J. & Urbach, H., Mumford–Shah model for one-to-one edge matching. *IEEE Transactions on Image Processing* **16** (2007), 2720–2732. [MR2472414](#)
24. Keeling, S. L. & Ring, W., Medical image registration and interpolation by optical flow with maximal rigidity. *Journal of Mathematical Imaging and Vision* **23** (2005), 47–65. [MR2208908](#)
25. Le Guyader, C. & Vese, L. A., A combined segmentation and registration framework with a nonlinear elasticity smoother. *Computer Vision and Image Understanding*, **115** (2011), 1689–1709. Special issue on Optimization for Vision, Graphics and Medical Imaging: Theory and Applications.
26. Mang, A. & Biros, G., Controlling the deformation map in diffeomorphic image registration. *arXiv:1503.00757v1*, 2015.
27. Miller, M. I., Christensen, G. E., Amit, Y. & Grenander, U., Mathematical textbook of deformable neuroanatomies. *Proceedings of the National Academy of Sciences* **90** (1993), 11944–11948. [Zb10788.92011](#)
28. Modica, L. & Mortola, S., Un esempio di  $\Gamma^-$ -convergenza. *Boll. Un. Mat. Ital. B (5)* **14** (1977), 285–299. [Zb10356.49008](#) [MR0445362](#)
29. Moreno, J. C., Prasath, V. B. S., Proença, H. & Palaniappan, K., Fast and globally convex multiphase

- active contours for brain MRI segmentation. *Computer Vision and Image Understanding* **125** (2014), 237–250.
30. Mumford, D. & Shah, J., Optimal approximation by piecewise smooth functions and associated variational problems. *Communications on Pure and Applied Mathematics*, **42** (1989), 577–685. [MR0997568](#)
  31. Ozeré, S. & Le Guyader, C., A joint segmentation-registration framework based on weighted total variation and nonlinear elasticity principles. In *IEEE International Conference on Image Processing (ICIP), 2014*, pages 3552–3556. IEEE, 2014. [MR3400024](#)
  32. Ozeré, S. & Le Guyader, C., Nonlocal joint segmentation registration model. In J.-F. Aujol, M. Nikolova, and N. Papadakis, editors, *Scale Space and Variational Methods in Computer Vision*, volume 9087 of *Lecture Notes in Computer Science*, pages 348–359. Springer International Publishing, 2015. [MR3394942](#)
  33. Pedregal, P., *Variational Methods in Nonlinear Elasticity*. SIAM, 2000. [Zb10941.74002](#) [MR1741439](#)
  34. Rabbitt, R. D., Weiss, J. A., Christensen, G. E. & Miller, M. I., Mapping of hyperelastic deformable templates using the finite element method. In *Proc. of SPIE*, volume 2573, pages 252–265, 1995.
  35. Rumpf, M. & Wirth, B., A nonlinear elastic shape averaging approach. *SIAM Journal on Imaging Sciences* **2** (2009), 800–833. [Zb11219.49035](#) [MR2540171](#)
  36. Unal, G., Slabaugh, G., Yezzi, A. & Tyan, J., Joint segmentation and non-rigid registration without shape priors. Technical Report SCR-04-TR-7495, Siemens Corporate Research, 2004.
  37. Wang, W., Slepčev, D., Basu, S., Ozolek, J. A. & Rohde, G. K., A linear optimal transportation framework for quantifying and visualizing variations in sets of images. *International Journal of Computer Vision* **101** (2013), 254–269. [Zb11259.68222](#) [MR3021062](#)
  38. Wirth, B., *Variational methods in shape space*. Dissertation, University Bonn, 2009.
  39. Wyatt, P. P. & Noble, J. A., MAP MRF joint segmentation and registration. In T. Dohi and R. Kikinis, editors, *MICCAI*, volume 2488 of *LNCS*, pages 580–587, 2002. [Zb11028.68935](#)
  40. Yezzi, A., Zöllei, L. & Kapur, T., A variational framework for integrating segmentation and registration through active contours. *Medical Image Analysis* **7** (2003), 171–185.
  41. Yuan, J., Bae, E., Tai, X.-C. & Boykov, Y., A spatially continuous max-flow and min-cut framework for binary labeling problems. *Numerische Mathematik* **126** (2014), 559–587. [Zb11290.49060](#) [MR3164146](#)
  42. Zhu, L., Yang, Y., Haker, S. & Tannenbaum, A., An image morphing technique based on optimal mass preserving mapping. *IEEE Transactions on Image Processing*, **16** (2007), 1481–1495. [MR2465225](#)